Tripoli – Libya

School of Engineering & Applied Science

Department of Mechanical Engineering & Energies

Experimental Study of Local Forced Convective Heat Transfer to Boiling Flow (Two Phase Flow)

By: Abd- Elsalam Elmahde Shlabik

Supervisor: Prof. Dr. Mohammad Salaheddeen Zawia

A dissertation submitted to The
department of Mechanical Engineering & Energies
In conformity with the Department Requirements
As partial fulfilment for the Degree of Master of Science
(Power Engineering)

December 2014

ABSTRACT

Two-phase flows have received much attention in the past few decades due to its importance in the power and process industries. Consequently, there is a continuous need to enhance knowledge of the parameters affecting two-phase flows in piping systems. Although a significant body of knowledge on two-phase flow was generated, available experimental data tend to be limited to two-phase flow in small diameter pipes. Two phase flow and boiling heat transfer are very important to industry for the design and use of heat exchange equipment. More than 60% of industrial heat exchange processes involve two phase flow in one form or another. The two phase can occur in the tubular boiler, boiling water reactor, boiler blow-down system, waste heat boilers, condensers, distillation and water purification towers, and many others.

The local boiling convective heat transfer coefficients to two phase flow (boiling flow) are determine experimentally by using a flow boiling test rig. The experimental work covers different flow rates (24,30,and 35 l/min) with different void fractions, using a test section (40 cm) long , and (2.1 cm) in diameter. Also the work covers the possibility of using the heating probe and heat transfer to measure the flow rates (flow-meter). The results show that the increase of void fraction in the boiling flow increases the heat transfer coefficients. The flow is not bubble flow only, the bubble flow void fraction up to 20% after that the flow is plug flow up to 50%. Also the heat transfer coefficients increase with the increase of heat flux. And there is a possibility of using the heat transfer (heating probe) as flow meter for measuring flow rates of single phase flow at constant heat flux but it can not be used for two phase flow.

الملخص

التدفق ذو الطورين اخذ انتباه كبير جدا في العقود القريبة الماضية نتيجة لأهميته في محطات الطاقة والصناعات، بالتالي يتطلب تعزيز المعرفة والعوامل المؤثرة في هذا النوع من التدفق (ذو الطورين) في أنظمة الأنابيب. وبالرغم من وجود المعرفة النظرية الكافية لهذا النوع من التدفق، فإن المعلومات العملية والتجريبية تكاد تكون محدودة لتدفق ذو الطورين في الأنابيب ذات الأقطار الصغير.

التدفق ذو الطورين ومعامل انتقال الحرارة في مرحلة الغليان مهمين جدا لصناعة وتصميم واستخدام أجهزة التبادل الحرارى، وتوجد حوالي أكثر من 60% من عمليات التبادل الحراري الصناعية تتضمن تدفق ذو الطورين في شكل أو أخر. تدفق ذو الطورين من الممكن ان يحدث في الغلايات الأنبوبية، مفاعلات غليان الماء، جهاز الغليان الحرارى الاستهلاكي، المكثفات، أبراج تنقية وتقطير المياه، ..الخ.

تمت دراسة معاملات انتقال الحرارة بالحمل بالنسبة للغليان الموضعي لتدفق ذو الطورين عمليا باستخدام جهاز اختبار لسريان تدفق ذو طورين (ماء في حالة غليان).

التجارب العملية شملت معدلات تدفق مختلفة (24,30,35 ل/د) مع اختلاف نسبة البخار الى التدفق، باستخدام أنبوب اختبار (40 سم) طولا، (2.1 سم) قطراً. أيضا شملت الدراسة إمكانية استخدام انتقال الحرارة الموضعي لقياس معدلات التدفق (جهاز قياس التدفق flow meter).

ومن النتائج تبين ان زيادة نسبة البخار الى التدفق في تدفق الغليان يزيد من معاملات انتقال الحرارة. وان التدفق ليس تدفق فقاعي فقط، بل التدفق فقاعي يكون عندما تكون نسية البخار الى التدفق الكلي لا تزيد عن 20% وبعدها يكون التدفق (plug flow) الى حوالي 50%. أيضا معاملات انتقال الحرارة تزيد مع زيادة كمية الحرارة المتدفقة. وان امكانية استخدام انتقال الحرارة (قطب التسخين) لقياس معدلات التدفق لتدفق ذو طور واحد ممكنة عند ثبات كمية الحرارة المتدفقة ولا يمكن استخدام انتقال الحرارة في قياس التدفق ذو الطورين.

This thesis dedicated to the memory of my mother.

To my Father, my beloved family members,

my teachers and lectures, and all my colleagues and friends.

ACKNOWLEDGEMENT

Firstly I have to thank Allah for helping me to complete this work. Also, I want to thank my colleagues in the Military Engineering Faculty, because they have had contributed to this work for many months.

I would like to express my deep and sincere thanks to my supervisor Dr. ***Mohammad Salaheddeen Zawia*** for his invaluable guidance and direction. His constant inspiration and support as well as his creative influence on my present work and during my study.

The final grateful to academy of post graduate and also to whose support is sincerely appreciated.

Special thanks go to my close friends Ezzeddin Almabruk and Nori Addbashi for their help during the period of research in the Academy.

TABLE OF CONTENTS

Abstract ii
الملخص..iii
Dedication..iv
Acknowledgement..v
Table of contents..vi
List of figures..x
Nomenclature..xii

Chapter 1: Introduction

1. General Introduction……………..…………………………………..……..1
1.1 Industrial Importance……………………………………………………1
1.2 Two-Phase Flow in Pipe Lines……………………………………….1
1.3 Fundamentals of Two-Phase Flow in Pipes………………………….3
1.4 Fundamentals of Boiling……………………………………………..5
1.4.1 Pool boiling……………………………………………...6
1.4.2 Flow boiling……………………………………………..8
1.5 Types of Two-Phase Flow……………………………………………11
1.5.1 Co-current flow patterns in horizontal flow…………...11
1.5.2 Co-current flow patterns of upward flow in vertical tub……………………………………………………...13
1.5.3 Co-current flow patterns of downward flow in a vertical tube…………………………………………..…...14
1.6 Void Fraction……………………………………………………15
1.7 Homogeneous Flow……………………………………………...17
1.8 Boiling Heat Transfer……………………………………………17
1.9 Project Objective……………………………………………...18

Chapter 2: Lecture Survey

Lecture Survey……………………………………………………..19

Chapter 3: Experimental Work

3.1Design of the test rig…………………………………………………...30

3.2Experimental Procedures…………………………………………….34

3.3Instrumentation and Procedures……………………………………..35

3.3.1 Temperature Measurements……………………………35

3.3.2 Pressure Measurements………………………………...36

3.3.3 Volume Flow Rate Measurements……………………..36

3.3.4 Heat Flux Calculation …………………………………37

3.3.5 Void fraction Estimation ……………………….......37

3.3.6 Local Heat Transfer Coefficients………………………38

3.3.7 Simple of Calculation………………………………….38

Chapter 4: Results and Discussion

4.1Introduction…………………………………………………………40

4.2Influence of Flow Temperature and Flow Rate……………………...40

4.3 Influence of Void Fraction in the Flow……………………………..42

4.4 Influence of Water Temperature on the Heat Transfer Coefficient…44

4.5 Relation Between the Heat Transfer Coefficient and Temperature Different Between (T_w & T_{surf})………………………………………46

4.6 Influence of Void Fraction on Temperature Difference (T_w & T_{surf})………………………………………………………...47

4.7 Influence of Void Fraction in the Flow at Volume Flow Rate (24 & 30 L/min)…………………………………………………..48

4.8 Relation Between the Heat Transfer Coefficient and Temperature Different Between (T_{surf} -T_w)……………………………………………..48

4.9 Influence of Void Fraction on Temperature Difference (T_{surf} -T_w) at Volume Flow Rate (24 & 30 L/min)…………………………………...49

Chapter 5: Conclusions

Conclusions………………………...50

References...51

Appendices (A)

Table A.1 heat transfer coefficient correlation and water temperature at constant volume flow rate (24 L/min)…………………………...57

Table A.2 heat transfer coefficient correlations and different volume flow rate…………………………………………………………...57

Table A.3 influence of void fraction on heat transfer coefficient at volume flow rate(24 L/min)…………………………………………58

Table A.4 influence of void fraction on heat transfer coefficient at volume flow rate(30 L/min)…………………………………………58

Table A.5 the relation between heat transfer coefficient and water temperature at constant volume flow rate (24 L/min)………………58

Table A.6 the relation between heat transfer coefficient and water temperature at constant volume flow rate (30 L/min)……………...59

Table A.7 the relation between heat transfer coefficient and water temperature at constant volume flow rate (35 L/min)……………...59

Table A.8 the relation between heat transfer coefficient and temperature different between (T_w & T_{surf}) at volume flow rate (24L/min)……………………………………………………………59

Table A.9 the relation between heat transfer coefficient and temperature different between (T_w & T_{surf}) at volume flow rate (30L/min)……………………………………………………………60

Table A.10 the relation between temperature different between (T_w &T_{surf}) and void fraction at volume flow rate (24L/min)……………………………………………………………60

Table A.11 the relation between temperature different between (T_w & T_{surf}) and void fraction at volume flow rate (30L/min)……………………………………………………………60

Appendices (B)

Photo (B-1) void fraction 5% at Volume flow rate (24)…………….61

Photo (B-2) void fraction 7% Volume flow rate (24)……………….61

Photo (B-3) void fraction 9% Volume flow rate (24)……………….62

Photo (B-4) void fraction 11% Volume flow rate (24)……………...62

Photo (B-5) void fraction 13% Volume flow rate (24)……………...63

Photo (B-6) void fraction 14% Volume flow rate (24)……………...63

Photo (B-7) void fraction 15% Volume flow rate (24)……………...64

Photo (B-8) void fraction 5% at Volume flow rate (30)…………….64

Photo (B-9) void fraction 7% at Volume flow rate (30)…………….65

Photo (B-10) void fraction 8% at Volume flow rate (30)…………...65

Photo (B-11) void fraction 9% at Volume flow rate (30)…………...66

LISTS OF FIGURES

Figure (1.1) Typical boiling curve and heat transfer mechanisms in pool-boiling……………………………………………………………..7
Figure (1.2) Flow boiling in a uniformly heated circular tube…………….10
Figure (1.3) Flow patterns in horizontal flow...……………………………11
Figure (1.4) Flow patterns of upward flow in vertical tube ………………..13
Figure (1.5) Flow patterns of downward flow in a vertical tube…………...14
Figure (3.1.a) The designed experimental test rig is consist……………….31
Figure (3.1.b) details of test section……………………………………...32
Figure (4.1) the relation between heat transfer coefficient and water temperature at constant volume flow rate (24 L/min)……………………..41
Figure (4.2) the relation between heat transfer coefficient and different volume flow rate………………………………………………………41
Figure (4.3) influence of void fraction on heat transfer coefficient at volume flow rate(24 L/min)……………………………………………………42
Figure (4.4) influence of void fraction on heat transfer coefficient at volume flow rate(30 L/min)……………………………………………………43
Figure (4.5) the relation between heat transfer coefficient and water temperature at constant volume flow rate (24 L/min)……………………..44
Figure (4.6) the relation between heat transfer coefficient and water temperature at constant volume flow rate (30 L/min)……………………..45
Figure (4.7) the relation between heat transfer coefficient and water temperature at constant volume flow rate (35 L/min)……………………..45
Figure (4.8) the relation between heat transfer coefficient and temperature different between (T_w & T_{surf}) at volume flow rate (24L/min)……………..46

Figure (4.9) the relation between heat transfer coefficient and temperature different between (T_w & T_{surf}) at volume flow rate (30L/min)……………..46
Figure (4-10) the relation between temperature different between (T_w & T_{surf}) and void fraction at volume flow rate (24L/min)…………………………..47
Figure (4.11) the relation between temperature different between (T_w & T_{surf}) and void fraction at volume flow rate (30L/min)…………………………..47
Figure (4.12) influence of void fraction on heat transfer coefficient at volume flow rate(24 & 30 L/min)……………………………………………..48
Figure (4.13) the relation between heat transfer coefficient and temperature different between (T_{surf} -T_w) at volume flow rate (24 & 30 L/min)………...48
Figure (4.14) the relation between void fraction and temperature difference (T_{surf} -T_w) at volume flow rate (24 & 30 L/min)……………………………49

Nomenclature

$\left(\frac{dp}{dL}\right)_{GR}$	Pressure drop due to gravitational forces
$\left(\frac{dp}{dL}\right)_{F}$	Pressure drop due to fraction loss
$\left(\frac{dp}{dL}\right)_{ACC}$	Pressure drop due to acceleration
ρ	density of the liquid, (kg /m^3)
v	average liquid velocity, (m /s)
g	acceleration due to gravity, (m/s^2)
d	diameter of the pipe, (m)
f_m	the moody friction factor
N_{Re}	Reynold's number
α	void fraction
β	volumetric vapour quality
S	slip ratio
V_G	vapour velocity, (m/s)
V_L	liquid velocity, (m/s)
h_{tp}	heat transfer coefficient (two phase), (kW/m^2 K)
q''	the heat flux, (kW)
T_{sur}	wall temperature, (C^0)
T_w	the bulk fluid temperature, (C^0)
Q	volume flow rate, (L/min)
A	test section area, (m^2)
k	thermal conductivity of the aluminium, (W/m K)
x	the distance between the two location where the temperatures are measured
ΔT	the temperature difference between two location along the heating probe

INTRODUCTION

1.0 General Introduction

Two-phase flows have received much attention in the past few decades due to its importance in the power and process industries. Consequently, there is a continuous need to enhance knowledge of the parameters affecting two-phase flows in piping systems. Although a significant body of knowledge on two-phase flow was generated, available experimental data tend to be limited to two-phase flow in small diameter pipes. In the analysis of two-phase flow thermal-hydraulics, various formulations such as the homogeneous flow model, drift flux model, and two-fluid model have been proposed.

1.1 Industrial Importance

Two phase flow and boiling heat transfer are very important to industry for the design and use of heat exchange equipment. More than 60% of industrial heat exchange processes involve two phase flow in one form or another. The two phase can occur in the tubular boiler, boiling water reactor, boiler blow-down system, waste heat boilers, condensers distillation, and water purification towers, and many others.

1.2 Two-Phase Flow in Pipe Lines

The Phase is a separate part of heterogeneous body or system, such as solid, liquid, gas, or vapour. Thus the two-phase system contains a mixture of any two of these states, such as (i) gas-liquid flow, (ii) liquid-liquid flow, (iii) gas-solid flow and (iv) liquid-solid flow. Most of the work done in horizontal and vertical pipes have been for the flow of gas and liquid.

Two-phase flows are classified by the void (bubble) distributions. Basic modes of void distribution are bubbles suspended in the liquid stream, liquid droplets suspended in the vapour stream, and liquid and vapour existing intermittently. The typical combinations of these modes as they develop in flow channels are called flow patterns. The various flow patterns exert different effects on the hydrodynamic conditions near the heated wall, thus they produce different frictional pressure drops and different modes of heat transfer and boiling crises. Significant progress has been made in determining flow-pattern transition and modelling.

The microscopic picture of the flow in the proximity of the heated wall can be described in terms of two-phase boundary-layer flow. The macroscopic effect of a two-phase flow on the frictional pressure drop still relies on empirical correlations. Two-phase flow in a channel (or conduit) can hardly become fully developed at low pressure because of the shape change in large bubbles and the inherent pressure change along the channel, which continually change the state of the fluid and thereby change the phase distribution and flow pattern. Both of these observations suggest high complexity in adiabatic two-phase flow, where a local or point description is insufficient without knowledge of the previous "history" of the flow. Additional complexities are introduced by the hydrodynamic instabilities and the occasional departure from thermodynamic equilibrium between the phases.

The flow-pattern (or flow-regime) models improve some of the deficiencies of the above models by taking into consideration local variation of density and velocity for each flow regime separately. conservation equations are solved under the assumption of predetermined. The geometric patterns of flow, such as bubbly, slug, wavy, annular, etc.

1.3 Fundamentals of Two-Phase Flow in Pipes

Two-phase flow obeys the fundamental laws of fluid mechanics. However, due to the presence of momentum, heat and mass transfer between phases it is difficult to calculate the dynamic surface tension, viscosity and density of the two-phase mixture. Therefore, two-phase flow theories are usually developed from the concepts of single-phase flow. Using the laws of conservation of mass and momentum, the steady-state total pressure gradient for a single-phase fluid can be described as. [1]

$$\left(\frac{dp}{dL}\right)_{TOTAL} = \left(\frac{dp}{dL}\right)_{GR} + \left(\frac{dp}{dL}\right)_{F} + \left(\frac{dp}{dL}\right)_{ACC} \qquad (1\text{-}1)$$

Where,

$\left(\frac{dp}{dL}\right)_{GR}$ = Pressure drop due to gravitational forces (1-2)

$\left(\frac{dp}{dL}\right)_{F}$ = Pressure drop due to fraction loss (1-3)

$\left(\frac{dp}{dL}\right)_{ACC}$ =Pressure drop due to acceleration (1-4)

The pressure losses due to gravitational forces and acceleration in compressible fluids are given by the following equations.

$$\left(\frac{dp}{dL}\right)_{GR} = g * \rho * \sin\theta \qquad (1\text{-}5)$$

$$\left(\frac{dp}{dL}\right)_{ACC} = \rho * v * \left(\frac{dv}{dL}\right) \qquad (1\text{-}6)$$

Where,

$\rho =$ density of the liquid, Kg/m 3

v = average liquid velocity, m/s

g = acceleration due to gravity, m/s^2

For incompressible fluids, such as oil and water, in horizontal flow (where the pipe angle to the horizontal, θ, is zero) the pressure gradient due to these terms can be neglected. Thus, for a single-phase, incompressible fluid in horizontal and steady state flow Equation (1-1) reduces to

$$\left(\frac{dp}{dL}\right)_{TOTAL} = \left(\frac{dp}{dL}\right)_{F} \tag{1-7}$$

The pressure gradient due to irreversible frictional pressure loss can be obtained from the (Darcy-Weisbach, and Malinowsky) equation.

$$\left(\frac{dp}{dL}\right)_{F} = \frac{2 * f_m * \rho * v^2}{d} \tag{1-8}$$

Where,

d = diameter of the pipe, m.

f_m = the Moody friction factor.

The Moody friction factor, f_m, is a function of the Reynold's number in laminar flow, and a function of both the pipe wall roughness and the Reynold's number in turbulent flow. For well develop turbulent flow the friction factor is a unique function of the Reynold's number. The Reynold's number is a dimensionless group given by

$$N_{Re} = \frac{\rho * v * d}{\mu} \tag{1-9}$$

The relationship between the Reynold's number, roughness of the pipe and the friction factor for laminar and turbulent flows is given in the moody diagram. However, the standard relationships developed for laminar and turbulent flow friction factors can also be used.

For laminar flow,

$$f = \frac{16}{N_{Re}} \qquad (1\text{-}10)$$

For turbulent flow (Blasius equation),

$$f = 0.079 * {N_{Re}}^{-0.25} \qquad (1\text{-}11)$$

1.4 Fundamentals of Boiling

Boiling is defined as the process of phase changing the state of a substance from liquid to gas by heating it past its boiling point. Different types of boiling can be defined according to the geometric situation and to the mechanism occurring. Regarding the geometry, it is possible to distinguish between pool boiling, where the heat is transferred to a stagnant fluid, and flow boiling, where the fluid has a velocity relative to the heating surface.

The three different boiling heat transfer mechanisms are nucleate boiling, where heat is transferred by means of vapour bubbles nucleating, growing and finally detaching from the surface, convective boiling, where heat is conducted through the liquid and this one evaporates at the liquid-vapour interface without bubble formation, and film boiling, where the heat is transferred by conduction and radiation through a film of vapour that covers the heated surface and the liquid vaporizes at the vapour liquid interface. Nucleate boiling and film boiling may occur in both pool boiling and flow boiling, while forced convective boiling occurs only in flow boiling.

In addition, if the temperature of the liquid is below the saturation temperature, the process is called sub-cooled boiling, whereas if the liquid is maintained at the saturation temperature the process is known as saturated boiling.

1.4.1 Pool Boiling

Pool boiling is defined as boiling from a hot solid surface submerged in an extensive volume of liquid which, apart from any convection induced by the boiling process, is stagnant. The relationship between heat flux q" and the wall superheat ($\Delta T = T_{wall} - T_{sat}$) is known as the boiling curve, and qualitatively illustrated for saturated pool boiling in Figure (1.1), with the nature of vapour formation also depicted. [2]

Initially (O-A), as the heat rate to the surface is increased there's no bubble formation and heat is transferred by natural convection between the hot surface and the liquid-vapour interfaces. At a certain value of wall super-heat (A) bubble nucleation is initiated on cavities present on the heater surface. This condition is called onset of nucleate boiling (ONB). In liquids that wet the surface well, the onset of nucleation may be delayed (A'), for these liquids a sudden activation of a large number of cavities at an increased wall superheat causes a reduction in the surface temperature while the heat flux remains constant (A'-A"). After inception, the slope of the curve increases dramatically.

The discrete bubbles are released from randomly located active sites (A-B). At higher heat flux the density of active sites and the frequency of bubble release increase. Transition from isolated bubbles to fully developed nucleate boiling (B-C) occurs when bubbles at a given site begin to merge in the vertical direction and with bubbles from the neighbouring sites.

Further increasing the heat flux, intense evaporation near the bubble base leads to periodic dry patches on the surfaces that are rewetted by the surrounding liquid (C-D). This results in a reduction in the slope of the curve.

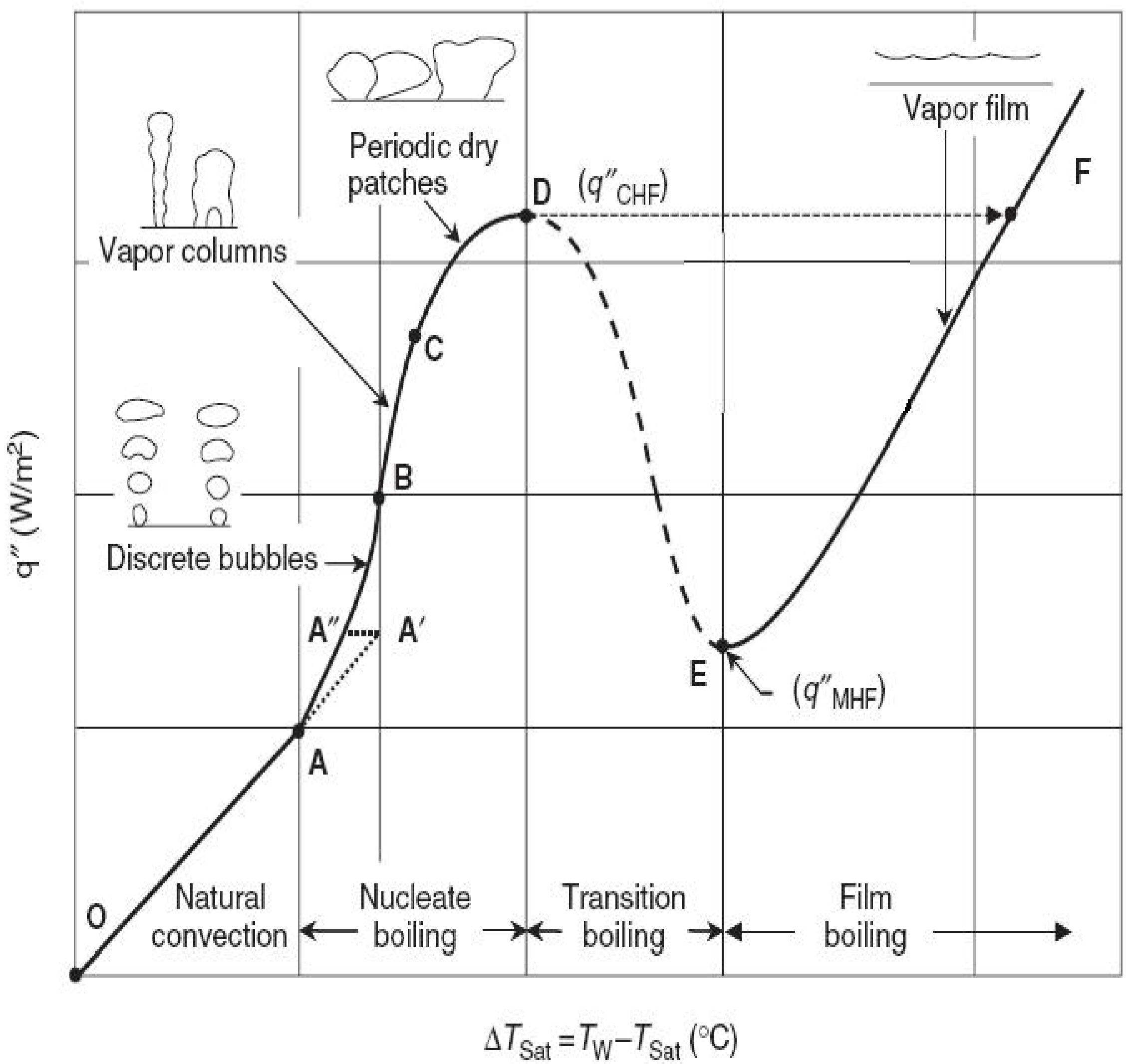

Fig (1.1) Typical boiling curve and heat transfer mechanisms in pool-boiling. [3]

Eventually, liquid is unable to rewet the heating surface and a large area becomes covered by a vapour blanket, causing a large temperature excursion on the heating surface (F), the heat flux corresponding to this condition (D) is known as the critical heat flux (CHF), and represents the upper limit of fully developed nucleate boiling or safe operation of equipment. If the temperature at (F) exceeds the melting temperature of the heating material, the heater will fail (burn out).

The curve (E-F) represents the stable film boiling, the surface is totally covered with vapour film and the liquid does not contact the solid, and the system can be made to follow this curve by reducing the heat flux,
with a reduction in heat flux in film boiling, a condition is reached when the vapour film can no longer be sustained and collapses. The heat flux corresponding to this condition (E) is called the minimum heat flux.

The region falling between nucleate and film boiling (D-E) is known as the transition boiling region. Transition boiling is very unstable and essentially inaccessible with constant heat flux boundary condition.

1.4.2 Flow boiling

A boiling curve similar to that in pool boiling is obtained when flow occurs inside a heated tube. The underlying mechanisms however, are more complex as the liquid-vapour flow configurations change due to the addition of vapour along the flow direction. Figure (1.2) shows a conceptual picture of forced flow boiling process, with qualitative temperature profile, for a circular tube with uniform heat flux boundary condition in which sub-cooled liquid enters the tube.

The first mode of heat transfer as sub-cooled liquid enters the tube is single-phase convection. The heat transfer coefficient in this region is constant except for the variations due property change with increasing liquid temperature in the flow direction.

Boiling will not occur until the wall temperature reaches a certain value (wall superheat) above the saturation temperature.

The primary formation of bubbles is known as onset of nucleate boiling, (ONB). Sub-cooled flow boiling exists when the bulk liquid temperature remains below its saturation value but the surface is hot enough for bubbles to form. Bubbles formed at the wall will condense as they move out of the developing saturation boundary layer, but the appearance of these bubbles will affect the heat transfer between the wall and the fluid. Initially, only few nucleation sites are active and a portion of the heat is transferred by single-phase convection between patches of bubbles.

As more nucleation sites are activated the contribution to heat transfer from nucleate boiling increases while the single-phase convective contribution diminishes. This region is termed partial nucleate boiling. When the surface becomes fully active for nucleation, fully developed nucleate boiling, is established. In addition, as the bulk fluid is heated the saturation boundary layer continues to grow and eventually covers the entire channel the saturated nucleate boiling region is reached. Further downstream, the addition of vapour to the flow leads to a transition in the heat transfer mechanism.

The thickness of the thin liquid film in annular flow is often such that the effective thermal conductivity is enough to prevent the liquid from being superheated to the temperature needed to sustain nucleate boiling. Heat is transferred from the wall by forced convection to the liquid-vapour interface, where evaporation occurs, temperature needed to sustain nucleate boiling.

The suppression of nucleate boiling indicates the beginning of the convective boiling region. Ultimately, at some critical vapour quality complete evaporation of the liquid film will occur.

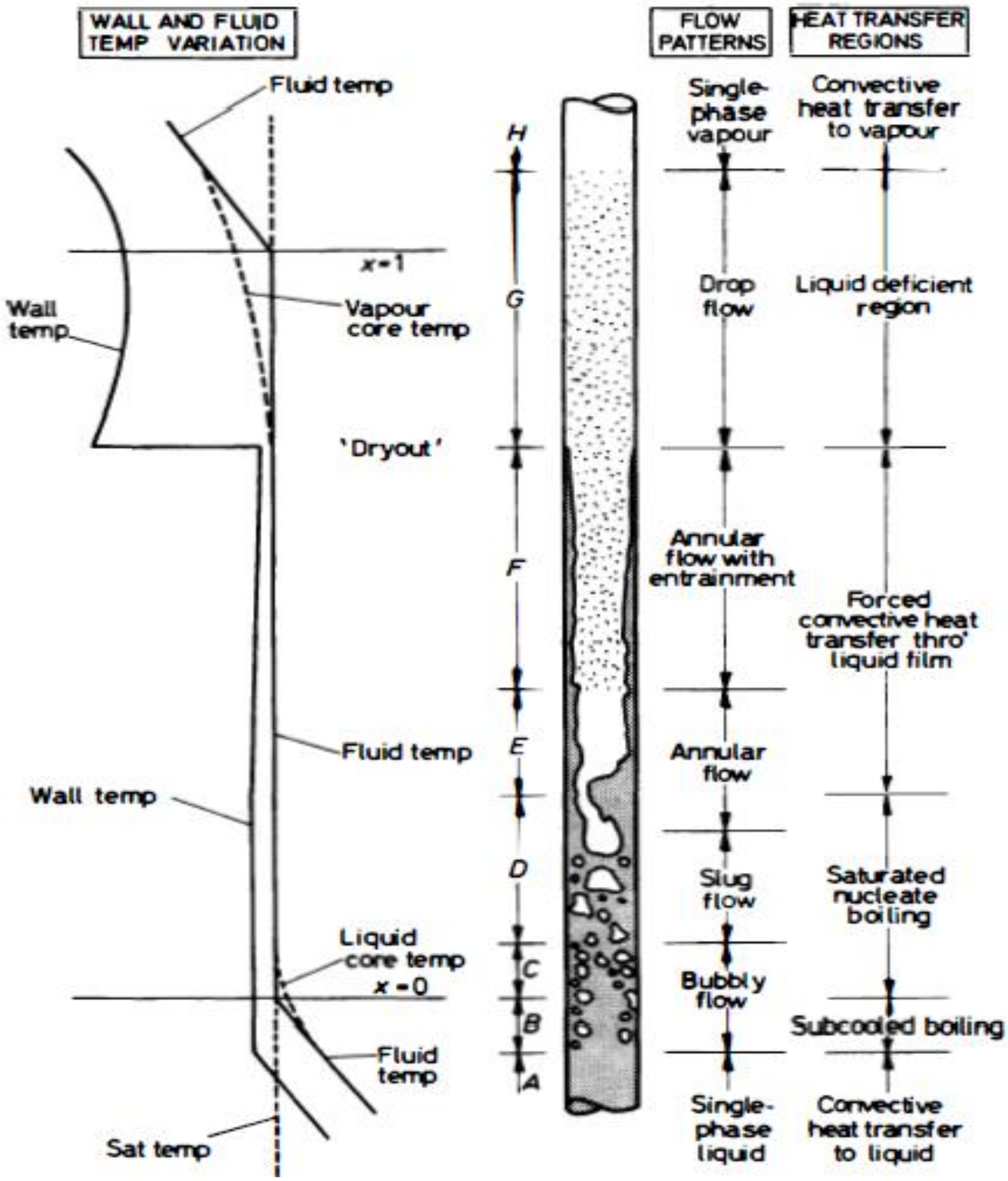

Fig 1.2. Flow boiling in a uniformly heated circular tube. [4]

This transition is known as dry out and is accompanied by a rise in the wall temperature. The area between the dry out point and the transition to dry saturated vapour is commonly referred to as the liquid deficient region.

1.5 Types Of Two-Phase Flow

Consider a two phase flow in a tube. When the two-phase flow in the same direction the flow is co-current flow. If they flow in opposite direction the flow is counter-current flow. But the concentration in this report will be placed on co-current flows.

1.5.1 Flow patterns in horizontal flow:-

The main types of flow patterns which exist are (a) Bubbly, (b) Plug, (c) Stratified, (d) Wavy, (e) Slug, (f) Annular. Fig(1.3) Shows the various flow patterns in horizontal flow of liquid and gas (Baker 1954 liquid and gas). [5]

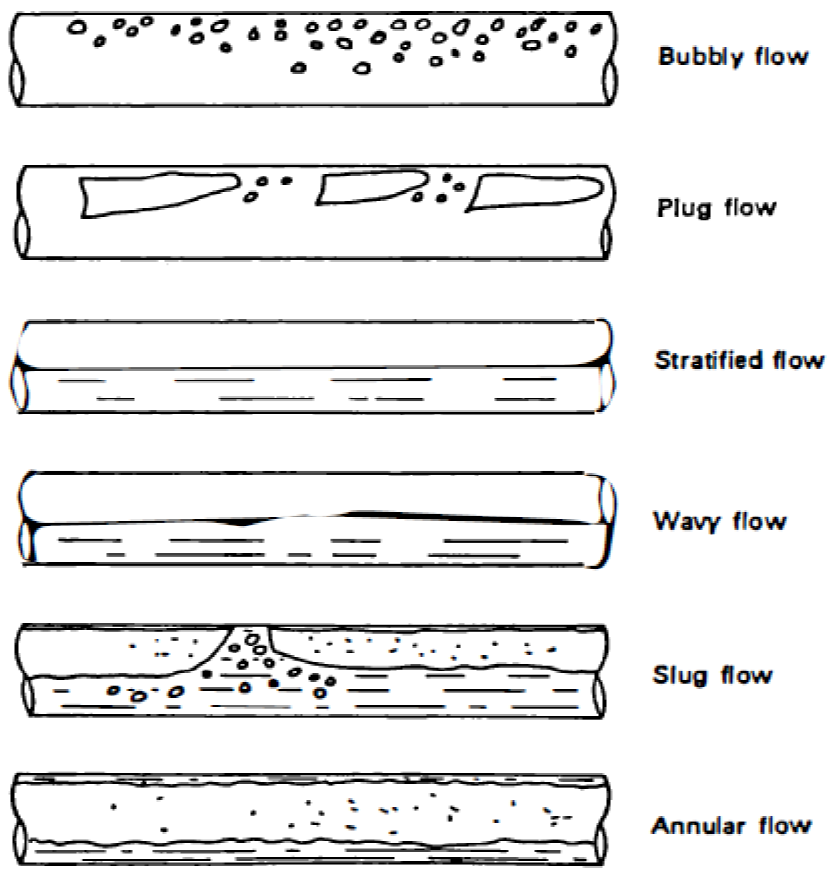

Fig (1.3) Flow patterns in horizontal flow

(a) Bubbly flow – Bubbles of gas or vapour are distributed in the continuous liquid phase. At low velocities the bubbles tend to move along the upper part of the duct, at moderate velocities they are fairly well distributed over the whole duct and at high velocities froth can occur.
(b) Plug flow – the bubbles of gas or vapour coalesce and alternate plugs of liquid and gas or vapour move along the upper part of the duct.
(c) Stratified flow – the two phases separate with the liquid flowing in the lower part of the duct. The gas or vapour in the upper part and with a relatively smooth interface. The pattern only occurs with low liquid and gas or vapour velocities.
(d) Wavy flow – in this pattern the gas or vapour moves at a higher velocity than the liquid and the interface in disturbed by waves travelling in the direction of flow.
(e) Slug flow – the waves are high and the summit of the waves seal the duct and from slugs moving with a higher velocity than the mean liquid velocity.
(f) Annular flow – the gas or vapour moves with relatively high velocity in the centre core of the duct surrounded by a liquid annular film along the duct wall, and it is thicker at the base of the duct.

1.5.2 Flow patterns of upward flow in vertical tube:-

The flow patterns are (a) Bubbly flow, (b) Slug flow, (c) Churn flow, (d) Annular flow, (e) Spray flow, as shown in fig (1.4).

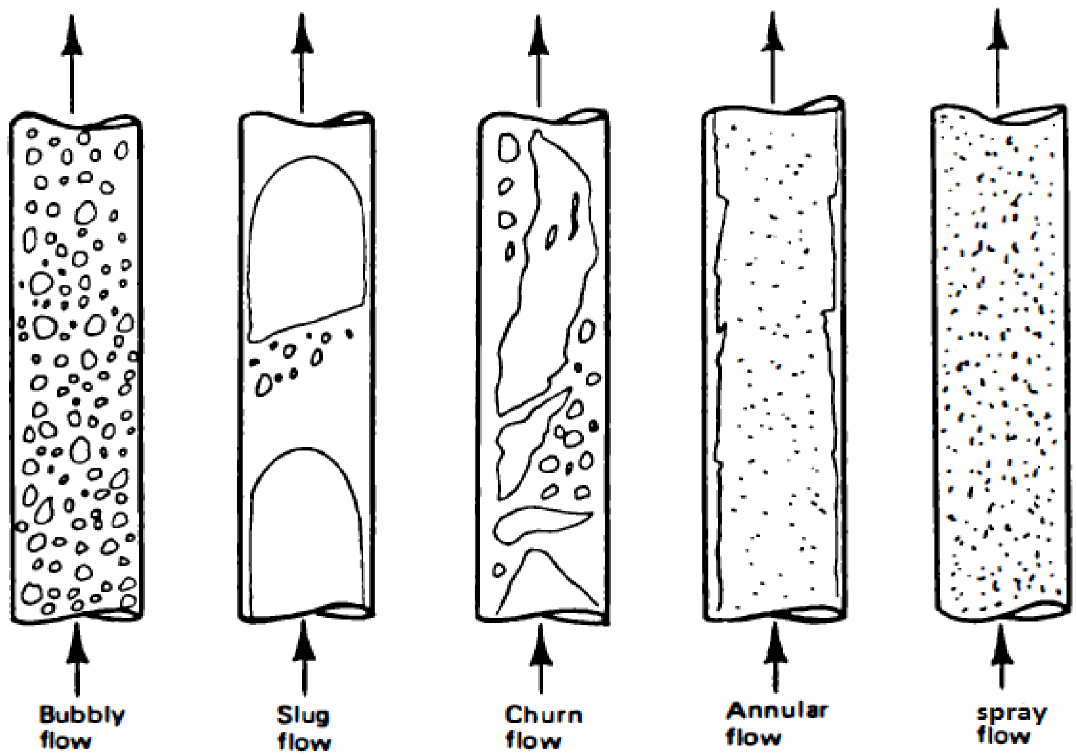

Fig (1.4) Flow patterns of upward flow in vertical tube

(a) Bubbly flow – the gas or vapour is distributed as bubbly in the liquid flow, the bubbles grow in size and tend to occupy the centre of the duct as the gas flow rate is increased or increased vaporisation.
(b) Slug flow – with further increase in gas or vapour the bubbles coalesce to form slug with a spherical cap, and are separated from the duct wall by a liquid film.
(c) Churn flow – in the centre of the duct the slug tend to unite with each other. And the liquid held up on the walls of the duct by the growing central core repeatedly collapse and fall back into the tube centre. This flow pattern is marked by severe pressure fluctuations.

(d) Annular flow – this flow is the same as in horizontal annular flow except the film thickness is the same around the tube.

(e) Spray flow – the liquid is entrained as droplets in the gas or vapour.

1.5.3 Flow patterns of downward flow in a vertical tube:-

The flow patterns are shown in fig (1.5) for air and water. The various flow patterns are (a) Bubble flow, (b) Slug flow, (c) Falling film, (d) bubbly falling film, (e) Churn flow, (f) Dispersed annular flow.

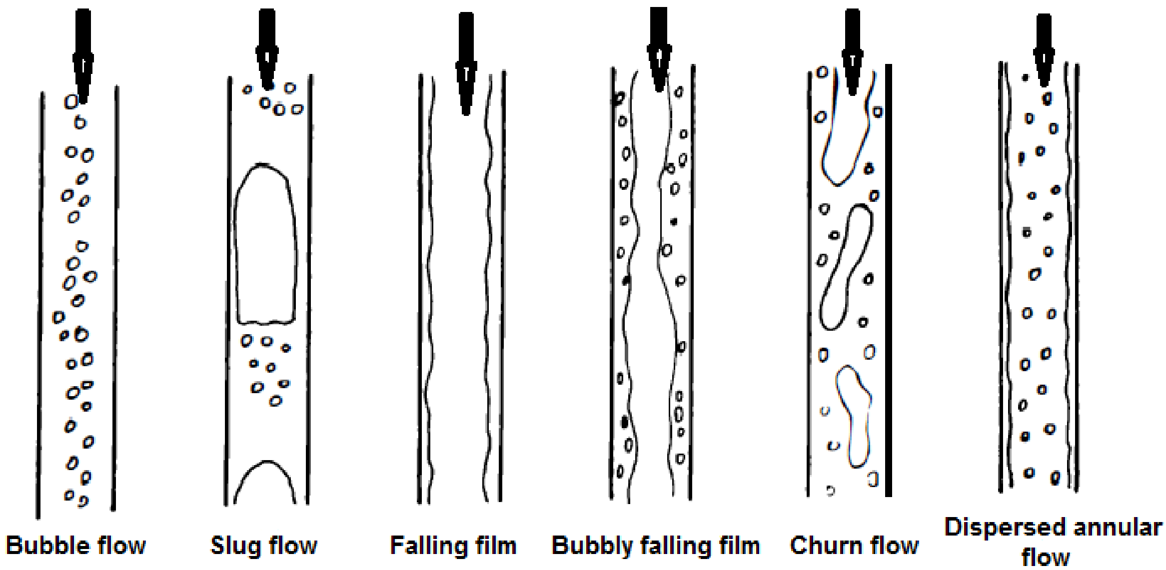

Fig (1.5) Flow patterns of downward flow in a vertical tube. [6]

(a) Bubble flow – bubble flow structure is quite different from the upward flow. The bubble in the downward flow gather near the pipe axis.

(b) Slug flow – when the gas or vapour flow rate is increased, the bubbles agglomerate into large gas packets. This slug flow is more stable than in the upward slug flow.

(c) Falling film – if the flow rates of the liquid and gas or vapour are very small the liquid film flows down the wall.

(d) Bubbly falling film – this flow patterns occur when the liquid flow rate is higher than gas flow rate. And bubbles are entrained within the film.

(e) Churn flow, and (f) Dispersed flow – when liquid and gas or vapour flow rates are increased a churn flow appears and can evolve into a dispersed annular flow.

1.6 Void Fraction

In a particular location and certain time of a tube where two-phase flow is moving, void fraction measures the amount of area occupied by the vapour (A_v), compared with the total cross-sectional area (A_{tube}) of the tube. [7]

$$\alpha = \frac{A_v}{A_{tube}} = \frac{A_v}{A_v + A_l} \qquad (1\text{-}12)$$

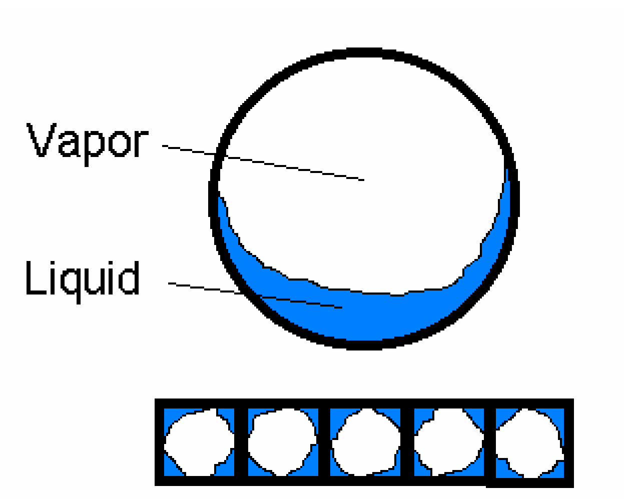

volumetric vapour quality

The volumetric vapour quality, β, or vapor volumetric flow ratio is defined as the ratio of vapour volumetric flow rate to the total volumetric flow rate; that is,

$$\beta = \frac{Q_G}{Q_G + Q_L} \qquad (1\text{-}13)$$

The relationship between a local (or static) quantity, (α), and a flow (or dynamic) quantity, (β), is

$$C = \frac{\propto}{\beta} \qquad (1\text{-}14)$$

or

$$C = \alpha + \frac{1-\alpha}{S} \qquad (1\text{-}15)$$

velocity

$$S = \frac{V_G}{V_L} \qquad (1\text{-}16)$$

In general, the quality and void fraction increase continuously along the channel, which implies the slip ratio also varies continuously along the channel. [8]

Three effects cause the vapour to slip

(1) The buoyancy effect-Being lighter than liquid, the bubble slips through the adjacent liquid that flows downstream.
(2) The velocity profile effect-For a convex flow velocity profile, for instance, in a steady bubbly flow, the centre line velocity is higher than the average velocity. With bubbles usually concentrating at the centre, they attain a higher velocity than the liquid.
(3) The Bernoulli effect-In a rapidly expanding flow, the two phases accelerate differently. For low initial velocities, the ratio of final velocities at the end of expansion, V_G/V_Lcan be approximated by $(\rho_G/\rho_L)^{1/2}$. [8]

1.7 Homogeneous Flow

If the liquid and vapour velocities are equal, then the slip ratio is one and the flow is said to be homogeneous. The flow is assumed to be homogeneous flow, i.e. v_v=v_l or S=1 (or the slip velocity(U_r) is neglected).

This assumption makes it relatively simple to treat two-phase mixtures effectively as single-phase fluids with variable properties.

Note that the assumption of homogeneous flow is very restrictive, and in fact accurate only under limited conditions (e.g. dispersed bubbly flow, mist flow). In general, a significant slip between the two phases is present, which requires the use of more realistic models in which v_v≠v_l. [9]

1.8 Boiling Heat Transfer

Boiling heat transfer is defined as a mode of heat transfer that occurs with a change in phase from liquid to vapour. There are two basic types of boiling, pool boiling and flow boiling. For modelling purposes, accurate heat transfer correlations are needed to properly design heat exchangers.

The boiling heat transfer coefficient is defined as:

$$h = \frac{q''}{T_w - T_{fluid}} \qquad (1\text{-}17)$$

where q'' is the heat flux from the wall of the solid substrate into the fluid, T_w is the wall temperature, and T_{fluid} is the bulk fluid temperature, which in saturated boiling is T_{sat}, the saturation temperature at the prevailing pressure P.

1.9 Project Objective

The objectives of the experiment are the fallowing:-

1- To study and understand types of two phase flow.
2- To determine the local boiling convective heat transfer coefficients for a flow boiling (two phase flow, water and vapor) down flow in tube.
3- To investigate the influence of the following:-
   i- Volume flow rate
   ii- Void fraction
   iii- Heat flux

   On heat transfer coefficients
4- To study the possibility of using a heating probe as a flow meter.

LITERATURE REVIEW

Visualization of boiling phenomena inside flow channels provides insight into bubble formation, coalescence, formation of slugs or plugs, and local dry-out conditions are all important in understanding the heat transfer phenomena. Although some of the heat transfer and pressure drop equations employed in the design of commercial equipment are derived from flow pattern-based models, the major benefit of flow pattern information lies in understanding the causes for premature dry-out or critical heat flux (CHF) condition in an evaporator. Another major benefit is in the design of the inlet and the outlet manifolds in multichannel evaporators. In recent years, a number of flow pattern maps have been developed for specific conditions such as small-diameter tubes, evaporation or condensation, and compact heat exchanger geometries. Earlier investigators extensively studied flow patterns for gas–liquid flows in channels with small hydraulic diameters.

Hewitt [9] notes that both evaporation and condensation processes have a significant effect on the flow patterns. The effect of evaporation on the flow pattern transitions was considered to be quite small in large-diameter tubes. This is one of the reasons why the flow pattern studies from gas–liquid systems, such as air and water, were extended to the case of evaporation. In smaller diameter tubes, the effect of evaporation could be quite dramatic. The evaporation of the liquid phase affects the flow in two ways. First, it alters the pressure drop characteristics by introducing an acceleration pressure drop component that can be quite large at higher heat fluxes. Second, the tube dimension is quite small, and the effect of surface tension forces becomes more important in defining the two-phase structure.

Mishima and Hibiki [10] developed one for an adiabatic air–water system in a 2.05-mm-diameter tube. The results indicate that the flow pattern maps developed for air–water flow are in general applicable, but the transition boundaries need to be refined for flow boiling in small-diameter tubes and channels.

Bonjour and Lallemand [11] report flow patterns of R-113 boiling in a narrow space between two vertical surfaces. The flow patterns observed are similar to those observed by other investigators : isolated bubbles, coalesced bubbles, and partial dry out. Comparing the bubble dimensions with the channel size is vital in determining whether the small channel size influences the bubble growth and leads to the confined bubble flow pattern.

Hestroni et al. [12] studied the evaporation of water in multichannel evaporators. The evaporators consisted of 21–26 parallel flow passages with channel hydraulic diameters of 0.103–0.129 mm. Hestroni et al. observed periodic behavior of the flow patterns in these channels. The flow changed from single-phase flow to annular flow with some cases of dry-out. The dry-out, however did not result in a sharp increase in the wall temperature. This clearly indicates that there is still some evaporating liquid. lm on the channel walls that could not be observed in the video-images.

In the study conducted by Lin et al. [13] air was introduced in a large mixing chamber upstream of the test section to reduce the disturbances resulting from gas injection. The presence of such low-pressure drop regions immediately before the test section leads to significant flow instabilities that cause large pressure drop excursions, and occasionally result in a negative pressure drop with a corresponding flow reversal in the channel.

The instability occurs in the negative-pressure-drop region of the demand curve plotted as the pressure drop versus inlet flow velocity of the sub-cooled liquid.

Kandlikar et al. [14] viewed the flow boiling of water in electrically heated multichannel evaporators consisting of six parallel channels. The flow structure was visualized using a high-speed video camera up to a maximum speed of 1,000 frames per second. The typical bubbly flow, slug flow, and annular flow patterns were observed. Nucleation was also observed in the bulk liquid as well as in the liquid (film). However, the most interesting discovery made, in an attempt to understand the severe pressure fluctuations (described later under Pressure Drop), was a visual confirmation of complete flow reversal in some of the channels.

Cornwell and Kew [15] conducted experiments in two sets of parallel channel geometries, 1.2 mm * 0.9mm deep, and 3.25mm *1.1mm deep. Their results indicate that the flow boiling in such small channels exhibits fully developed nucleate boiling characteristics in the isolated bubble region at lower qualities. At higher qualities (when the bubbles fill the entire cross section), and in the annular flow region, convective effects dominate heat transfer. These characteristics are similar to those observed for the large-diameter tubes. The isolated and confined bubble regions exhibit characteristics similar to the nucleate boiling-dominant region, while the annular-slug region exhibits the convective dominant trend seen in large-diameter tubes

Lin et al. [16] obtained flow boiling data with R-141b in 1-mm-diameter tubes. Their results indicate that the heat transfer coefficient exhibits behavior similar to that reported by Cornwell and Kew [15].

The role played by bubbles is clearly an important one. Specifically, they presented detailed results at G D 500 kg/m^{2}s with q from 18 to 72 kW/m^2. At high heat fluxes, they observed considerable fluctuations in the wall temperature readings indicative of flow oscillations that cause changes in the instantaneous values of local saturation temperature and heat transfer rate.

Wambsganss et al. [17] conducted extensive experiments on flow boiling of R-113 in a 2.92-mm-diameter tube. Their results indicate that the heat transfer coefficient was sensitive to both heat flux and mass flux changes, except for the lowest mass flux result.

Mertz et al. [18] conducted extensive experiments with water and R-141b boiling in six different mini-channel configurations. The flow boiling was observed as oscillatory phenomena in multi-channels. It is interesting to note that although the heat transfer coefficient increased with heat flux in almost all cases for single channels. For all channels in multichannel configuration, the heat transfer coefficient decreased with increasing heat fluxes. It is suspected that the flow oscillations and reversals observed in multi-channels are responsible for the degradation in heat transfer. For R-141b boiling in multichannel configuration, the heat flux effects were weak and somewhat mixed.

Rivera & Xicale [19] studied Heat transfer coefficients in two phase flow for the water/lithium bromide mixture used in solar absorption refrigeration systems, and described that the experimental results which obtained from the heat transfer coefficient in saturated nucleate boiling for water / lithium bromide mixture flowing upward in a uniformly heated vertical tube. It is observed that the average of heat transfer coefficient increased with increasing of heat flux and with the decrease of the concentration and the temperature difference.

Karslia et al. [20] visualized the study on the effect of heat transfer enhancement on flow instabilities in forced convection boiling in horizontal tube .there are five different heat transfer surface configurations and five different inlet temperatures are used to observe the effect of heat transfer enhancement and inlet sub-cooling. All experiments are carried out at constant heat input, system pressure and exit restriction. Dynamic instabilities, namely pressure-drop type, density-wave type and thermal oscillations are found to occur for all the investigated temperatures and enhancement configurations. The effect of the enhancement configurations on the characteristics of the boiling flow dynamic instabilities is studied in detail. The comparison between the bare tube and the enhanced tube configurations are made on the basis of boiling flow instabilities. Differences among the enhanced configurations are also determined to observe which of them is the most stable and unstable one. The amplitudes and periods of pressure-drop type oscillations and density-wave type oscillations for tubes with enhanced surfaces are found to be higher than those of the bare tube. The bare tube is found to be the most stable configuration, while tube with internal springs having bigger pitch is found to be the most unstable one among the tested tubes.

It's found that system stability increases with decreasing equivalent diameter for the same type heater tube configurations; however, on the basis of effective diameter there is no single result such as stability increase/decrease with increasing/decreasing effective diameter.

Ghiaasiaan and Chedester [21] analyzed the boiling incipience of water in micro channels (the tube with diameter of 0:1 – 1 mm range). Macro-scale models and correlations appear to under predict the heat fluxes that lead to the boiling incipience in micro-tubes. It is suggested that boiling incipience in micro channels may be controlled by thermo capillary force that tends to suppress the micro bubbles which form on wall cavities. Accordingly, a semi-empirical method is proposed for predicting the boiling incipience in micro-tubes. The effect of the turbulence characteristics of the micro-tube on the proposed method is also examined.

Measurement and prediction of saturated flow boiling heat transfer in a water-cooled micro-channel heat sink are studied by Qu, and Mudawar [22] Then the results provided new physical insight in to the unique nature of flow boiling in narrow rectangular micro-channels. micro-channels contain 21 parallel channels. The tests were performed with deionized water over mass velocity range of 135-402 kg/m^2, inlet temperature of 30 and 60 ^{o}C , and inlet pressure 1.17 bar. then the results indicate an abrupt transition to annular flow near the point of zero thermodynamic equilibrium quality, and heat transfer coefficient is shown to decrease with increasing thermodynamic equilibrium quality .

Wang et al. [23] studied the two phase flow pattern in small diameter tubes with the presence of horizontal return bend . and observed of the tow phase flow pattern for air water mixtures inside 6.9 , 4.95 and 3 mm smooth diameter tubes. The influence of the return bend on two phase flow are investigated for a mass flux of 50 kg/m^{2}s having quality less than 0.1, no influence on the flow patterns is seen at larger curvature ratio of 7.1, where the curvature ratio reduced to 3, the flow pattern is temporarily turned from stratified flow to annular flow. This transition phenomenon is related to the surface tension and reduction of the length of swirl flow.

Hibiki & lshii [24] researched about one dimensional drift flux model for two phase flow in large diameter pipe and viewed that the practical importance of the drift flux model for two phase flow analysis in general and in the analysis of nuclear reactor transients and accidents, the distribution parameters and the drift velocity have been studied for vertical upward tow phase flow in large diameter pipe. One of the important flow characteristics in large diameter pipe is a liquid recirculation induced at low mixture volumetric flux and also affect the liquid velocity profile and the formation of cap or slug bubbles, the distribution parameters and the drift velocity in large diameter pipe different from those in of inlet flow regime dependent drift flux correlation have been developed for two phase flow in large diameter pipe at low mixture volumetric flux. A comparison of newly developed correlations with various data at low mixture volumetric flux shows a satisfactory agreement as the drift flux correlation in large diameter pipe at high mixture volumetric flux, the drift flux correlations developed by kataoka- Ishii , and Ishii have been recommended for cab bubbly flow, churn and annular flows, respectively, based on the comparisons of the correlations with existing experimental data.

Huai et al. [25] they conducted an experimental study of boiling heat transfer and pressure drop of carbon dioxide (CO_2) flowing in multiport extruded aluminum test section. (CO_2) was heated by hot water flowing inside copper blocks that were attached at both sides of test section. The results indicate that pressure drop along the test section is very small, the phase (CO_2) flow exhibits a higher heat transfer coefficient than that of single phase liquid or vapor, and show that the mass velocity heat flux effects on flow boiling heat transfer.

Lee and Mudawar [26] studied the phase flow in high heat flux micro channel heat sink for refrigeration cooling applications and concerning two phase flow and heat transfer of R134 in micro channel incorporated as evaporator in refrigeration cycle. Boiling heat transfer coefficients were measured by controlling heat flux (q"=15.9-93.8 W/cm^2) and vapor quality (xe=0.26-0.87) over broad range of mass velocity. While prior studies point to either nucleate boiling or annular film evaporation as dominant heat transfer mechanisms in small channels, the studies show that the heat transfer is associated with different mechanisms for low qualities ($xe< 0.05$) corresponding to very low heat fluxes, and high fluxes produce medium quality ($0.05<xe<0.55$) or high quality ($xe > 0.55$) flows dominant by annular film evaporation. A new heat transfer coefficient correlation is recommended which show excellent predictions for both R134 and water.

An experimental study associated with two phase flow and heat transfer during flow boiling in two vertical narrow annuli has been conducted by Changhon et al. [27] the parameters examined were : mass flux from 38.8 to 163.1 kg/m^{2}s, heat flux from 4.9 to 50.7 kW/m^2 for inside tube and from 4.2 to 78.8 kW/m^2 for outside tube; equilibrium mass quality from 0.02 to 0.88, system pressure from 1.5 to 6.0MPa. It was found that the boiling heat transfer was strongly influenced by heat flux, while the effect of mass velocity and mass quality were not very significant. This suggested that the boiling heat transfer was mainly via nucleate boiling. The data were used to develop a new correlation for boiling heat transfer in the narrow annuli. In the two-phase flow study, the comparison with the correlation of Chisholm, Mishima et al, indicated that the existing correlations could not predict the two-phase multiplier in the narrow annuli well. Based on the experimental data.

Hetsroni et al. [28] visualized the flow pattern and measured heat transfer coefficient during explosive boiling of water in parallel triangular micro channels. The flow visualization showed that the behavior long vapor bubbles, occurring in micro channel at low Reynolds number, was not similar to annular flow with interposed intermitted slugs of liquid between two long vapor trains. In the presence of the two phase liquid vapor flow in the micro channel, there are pressure drop oscillations, which increase with the increasing of vapor quality, and strong dependence of heat transfer coefficient on vapor quality. The time when liquid wets the heated surface decrease with increasing heat flux, dry out occurs immediately after venting of elongated bubble .

Changhon et al. [29] Studied two phase flow and heat transfer during flow boiling in to vertical narrow annuli. it was found that the boiling heat transfer influenced by heat flux , while the effect of mass velocity and mass quality were not very significant. some characteristics of air water two phase flow in small diameter indicated that the existing correlations not predict the two phase multiplier in the narrow annuli well.

A comprehensive experimental single-phase flow and saturated flow boiling heat transfer and pressure drop study has been carried out by Owhaib [30] on vertical stainless steel tubes with inner diameters of 1.700, 1.224 and 0.826 mm, using R-134a as the test fluid. The heat transfer and pressure drop results were compared both to conventional correlations developed for larger diameter channels and to correlations developed specifically for micro-scale geometries. Contrary to many previous investigations, this study has shown that the test data agree well with single-phase heat transfer and friction factor correlations known to be accurate for larger channels, thus expanding their ranges to cover mini/micro-channel geometries.

The main part of the study concerns saturated flow boiling heat transfer and pressure drop. Tests with the same stainless steel tubes showed that the heat transfer is strongly dependent on heat flux, but only weakly dependent on mass flux and vapor fraction (up to the location of dryout). This behavior is usually taken to indicate a dominant influence of nucleate boiling, and indicates that the boiling mechanism is strongly related to that in nucleate boiling. The test data for boiling heat transfer was compared to several correlations from the literature, both for macro- and mini-channels.

A new correlation for saturated flow boiling heat transfer of refrigerant R-134a correlation was obtained based on the present experimental data.

Krishnamurthy and peles [31] studied flow boiling of water in circular staggered micro-pin fin heat sink. The local temperature measurements are used to elucidate the two phase heat transfer coefficients. The flow is visualized as vapor slug and annular flow pattern . a flow map is constructed and compared with maps of adiabatic micro scale systems and good agreement is observed. A model for two phase heat transfer coefficient in convective boiling regime is developed. frictional multiplier from micro scale studies is used to define the enhancement factor in the heat transfer coefficient model and reasonable agreement is obtained between experiments and prediction .

An experimental study is carried out on critical heat flux for flow boiling of R134 in single circular micro tubes by Ndao et. al [32] the experiments are conducted over large range of mass flux, inlet sub-cooling, saturation pressure, and vapor quality.

CHF occurred at high qualities and increased with increasing mass flux and inlet sub cooling. CHF generally but not always decrease with increasing the saturation of pressure and vapor qualities.

EXPERIMENTAL WORK

3.1 Design of the Test Rig

The test rig is designed to provide high drop in system pressure in order to form two phase flow (flow boiling) at low saturation temperature. This type of boiling is termed flash boiling. The pressure drop is occurred by the height of the rig, and the difference in diameters between the connecting pipes and the test section. The rig dimensions are 6 meter in height and 25.4mm in diameter except the test section which is 21mm diameter. The test section is fitted to the rig in the down flow section. The first design of the rig was shorter and the test section was fitted to the upward section. Because the pressure drop was not enough to allow flow boiling the height of the test rig is increased to 6 meter to provide higher pressure drop. But still there is no boiling and the pressure increased with the temperature of the flow.

To check what is happening in the down comer section of the test rig, a glass pipe is fitted in the down comer section to see the flow. The flow is found to be two phase flow i.e. boiling occurred and with different ranges of void fraction. Therefore the test section is transferred to the downward side and the test rig finally designed as shown in fig (3-1).

The designed experimental test rig is consist of :-

(i) Water Pump
(ii) Flow Meter
(iii) Control Valve
(iv) Test Section
(v) Electric Heaters
(vi) Water Tank
(vii) Connecting Pipes

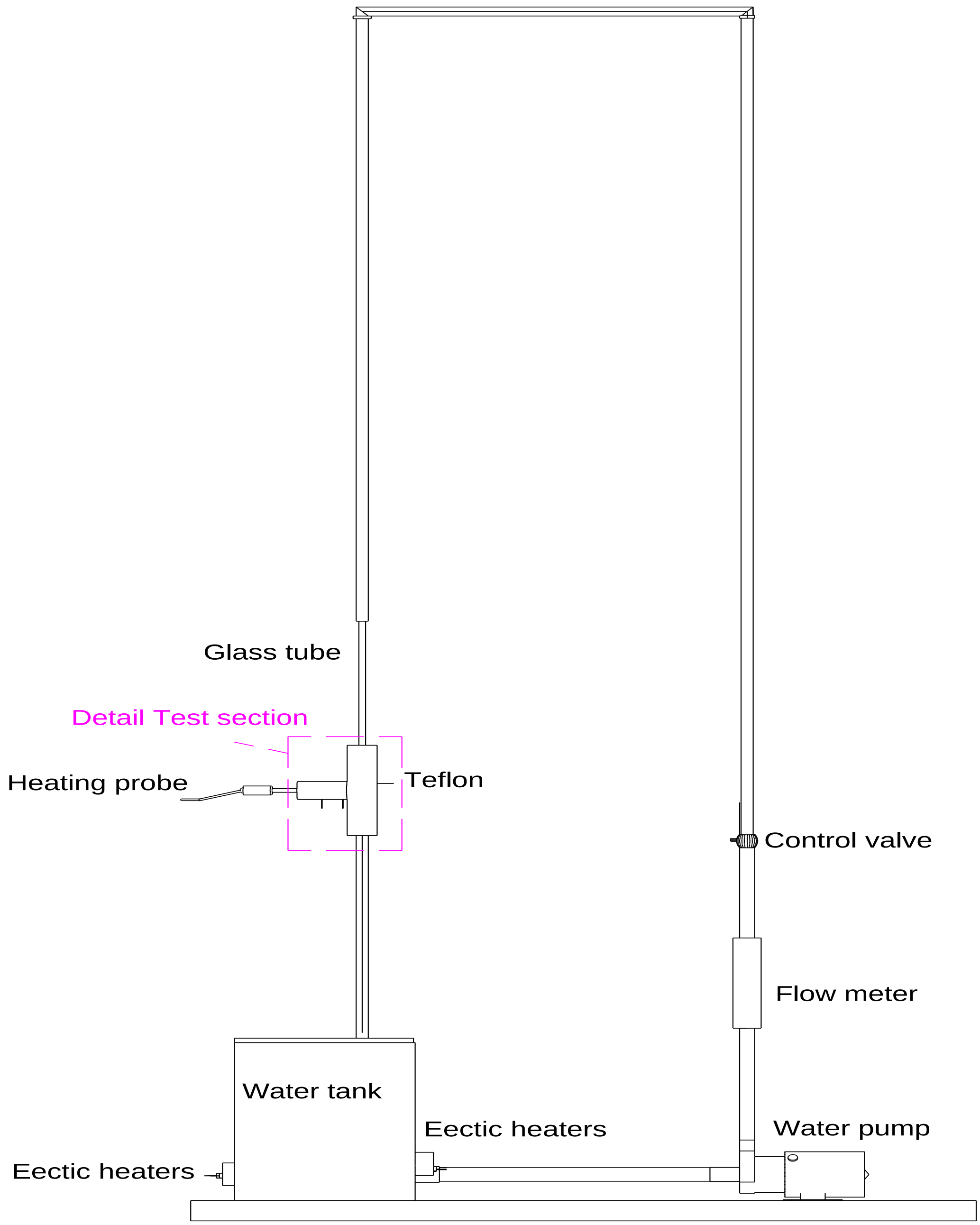

Sematic diegram test rig

Fig (3.1.a) The designed experimental test rig is consist

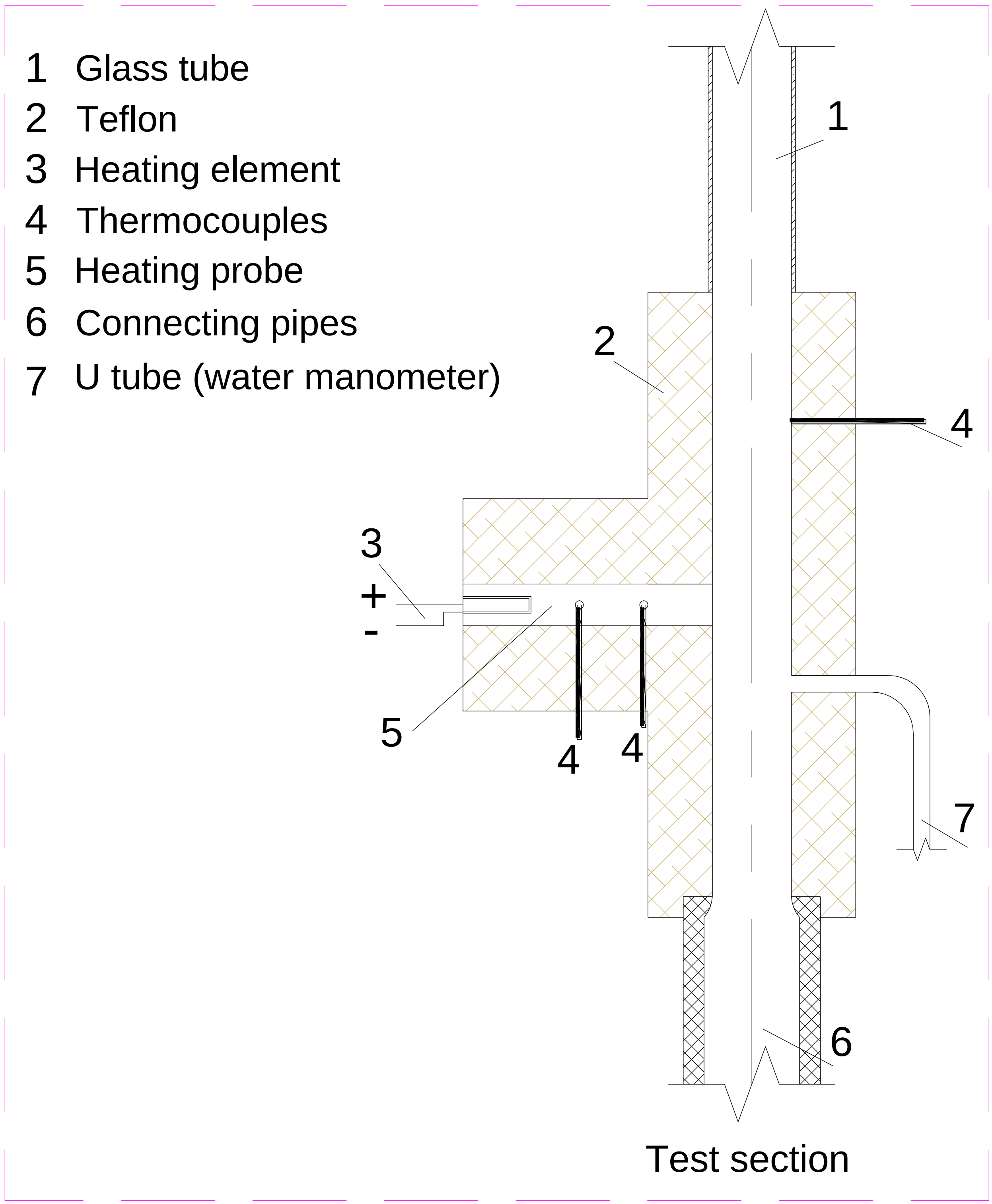

Detail Test section

Fig (3.1.b) details of test section

- Pump:- The water pump type of (centrifugal pump, the pump is of the high speed centrifugal type manufactured "Stuart Turner", at maximum speed the pump flow rate is 50 litres per minute) is used to circulate the water through the system.
- Flow Meter:- Flow meter is used to measure the flow rate of the water flowing through the test rig. It is fitted to the rig above the pump as showing in the figure (3.1.a). The type of the flow meter is Rotameter P6108. The flow meter will give direct readings of the flow rates to individual experiments.
- Control valve:- There is one control valve attached to the rig as shown in fig (3.1.a). It is used for controlling the volume flow rate and the pressure in the rig.
- Test Section:- The test section is the most important part in the rig, where all the measurements are taken. It consist of two parts, the first part is made of a glass tube, it is 0.4 meter long and 21mm in diameter. The second part made of a Teflon where, the heating probe, U tube, and thermocouples are attached to the test section as shown in fig (3.1.b).

(a) The heating probe is made of an aluminium bar of 10 mm diameter and 60 mm long. An electric heating element is fitted to one end which provides power of 80 watts. The other end of the aluminium bar is attached to the test section as a part of the inside surface of the test section tube as shown in fig (3.1.b). The heating probe is insulated by insulated wool to prevent heat loss to the surroundings.

(b) The U tube is fitted to the test section as shown in fig (3.1.b) in order to determine the pressure in the test section.

(c) Thermocouples type (N type, nisil -, nisrosil +) are used for measuring the temperatures. They are attached to the heating probe as shown in fig (3.1.b). Holes are drilled to the centre line of the aluminium bar and the two thermocouples are inserted in the holes and glued with Araldite. The two thermocouples are used to measure the temperatures along aluminium bar to calculate the heat flux and wet end surface temperature of the heating probe. A thermocouple is fitted to the test section at the Teflon part to measure the temperature of the flow.

- Electric Heaters:- Four electric heaters, two are (2 kW) power and the other two are (1 kW) power are fitted to the tank to preheat the water inside the tank before pumping it through the system.
- Connecting pipes:- Pipes of 25.4 mm diameter were used for connecting the above equipment to complete the rig, see fig (3.1.a).

3.2 Experimental Procedures

Local boiling convective heat transfer coefficients are determine experimentally by using the flow boiling test rig shown in fig(3.1.a). The experimental procedure covers different flow rates(24,30,and 35L/min) with different void fractions, using a test section (40 cm) long , and (2.1 cm) in diameter.

First the water is boiled in the tank to get rid of the dissolved gases in the water, to ensure that all the bubbles in the flow boiling are water vapour bubbles only. Second, heat is added to the water in the tank up to a temperature of ($84C^0$) at atmospheric pressure, using four electric heaters. Then the pump is turn on and the water flows throughout the test rig.

The vapour formation in the flow (bubble formation) is obtain when the hot water is superheated due to pressure drop in the test rig. To increase the pressure drop, the diameter of test section is made smaller than the connecting pipes of the test rig. In order to increase the amount of vapour in the flow the water temperature in the tank is increased.

A number of experiments are carry out for flow rates (24, 30, 35 L/min), each flow rate has different void fraction. The void fraction is change by increasing the water temperature in the tank in order to increase the superheat of the flow when it reach the test section to procedure more vapour .

3.3 Instrumentation and Procedures

The measuring equipment are switched on well in advance in order to stabilize them before taking the measurements. The flow rates are controlled by means of a valve fitted after the flow meter which measures the flow rates. The heating probe is switched on for supplying heat flux to the flow. A number of thermo-couples are used for temperature measurements, two of the temperatures are the temperatures along the aluminium bar of the heating probe fig (3.1.b). They are used to find out the heat flux that transferred to the flow, and to deduce the wet end surface temperature of the heating probe.

3.3.1 Temperature Measurements

The flow temperature and the temperatures along the heating probe were measured by means of two calibrated thermocouples. A circuit diagram of the system which is used for measuring the temperature is shown in fig (3.1.b). It consists of two thermocouples, and digital reading system.

The two thermocouples attached to the heating probe at distances from the surface of the probe in contact with the flow. 16mm, 17mm. Holes were drilled to the centre line of the probe, then the thermocouples are placed inside the holes and glued. The thermocouples are connected to digital reading system.

The temperature of the surface of the probe in contact with the flow cannot be measured directly. A simple calculation is needed to calculate it using the temperatures measured along the heating probe. See the results analysis.

3.3.2 Pressure Measurements

The pressure is measured by means of U tube water manometer. The U tube manometer measured the pressure difference between the pressure inside the test section and the room.

3.3.3 Volume Flow Rate Measurements

The volume flow rate is measured by means of a flow meter. It is placed above the pump in upward section. The flow through the flow meter was single phase liquid. The flow meter gives the volume flow rate in (L/min). Then the velocity of the flow can be calculated by.

$$Q = A * u \tag{3-1}$$

$$\therefore u = Q/A \tag{3-2}$$

The velocity of the flow is increased in the test section by decreasing the tube diameter there for the pressure in the test section decreases.

3.3.4 Heat Flux Calculation

Since there was some heat lost from the heating probe to the surrounding, the surface heat flux could not be measured directly by wattmeter, therefor the heat flux was calculated using equation

$$\ddot{q} = \frac{q}{A} = \frac{k}{x}\Delta T \qquad (3\text{-}3)$$

The temperature distribution along the heating probe was measured, and the thermal conductivity of the aluminium taken as a constant at the average temperature along the bar.

Where (k) is the thermal conductivity of pure aluminium at the average temperature (W/m K), (ΔT) the temperature difference between two location along the heating probe (K), (x) the distance between the two location where the temperatures are measured.

3.3.5 Void Fraction Estimation

The method used to determine the vide fraction using speed camera (photographic).

A high speed camera (Canon) is used to determine the void fraction of flow boiling. During each experiment some photographs are taken for the flow through the glass tube just before passes the heating probe. Some of the photographs are taken for different regimes, see the photos in appendix (B). Void fraction calculations: -

The void fraction is the ratio of the vapour area flow rate to the total area flow rate

$$\alpha = \frac{A_v}{A_v + A_l} \qquad (3\text{-}4)$$

From the photographs, the number of bubbles and their diameters were determined for certain area. The area of each bubbles calculated by

$$A_B = \pi \frac{D^2}{4} \tag{3-5}$$

The total area of the vapour is the sum of the bubbles areas (m^2).

3.3.6 Local Heat Transfer Coefficients

The local heat transfer coefficients of two phase flow (h_{tp}) are calculated from the definition

$$h_{tp} = \frac{\ddot{q}}{\Delta T} \tag{3-6}$$

Where ($\ddot{q}$) local heat flux at the end surface of the heating probe and (ΔT) the difference between the surface temperature and the flow temperature.

3.3.7 Sample of Calculation

Some assumptions were taken in order to simplify the calculations.

The assumptions are the following:-

1- The heat flux flow lines in the aluminum bar of the heating probe were straight lines along the bar (one dimension).

2- The transferred heat flux to the water was the same heat flux flows between the thermocouples i.e. no heat losses to the surroundings from the end of the heating probe.

3- The temperatures were equal over the wet end surface area of the heating probe.

4- The two phase flow is co-current flow, uniform and study, the flow is homogeneous that is the velocity of the bubbles was the same velocity of the liquid (no slip).

5- The bubbles assumed to be a spherical shape.

6- The void fraction estimation, from photo (B-1) the tube is divided into number of parts and the void fraction is estimated for each part by dividing the bubbles area to the total area the flow then by taking the average, the void fraction is (5%).

Heat flux calculation

K= 0.270 (kW/m K) , $\Delta x = (x_1 - x_2) = 0.016$ m , $r = x_2/x_1 = 0.5$

$\Delta T = (T_1 - T_2)$

T1	T2	Tw
162	125	84

$$\ddot{q} = \frac{q}{A} = \frac{k}{x} \Delta T$$

$$\frac{q}{A} = 607.500\ (\frac{kW}{m^2})$$

- **Temperatures calculation**

$$T_{surf} = \frac{T_2 - T_1 r}{1 - r}$$

$$T_{surf} = 60$$

- **Two phase heat transfer calculation**

$$h_{tp} = \frac{\ddot{q}}{\Delta T}$$

$$h_{tp} = \frac{\ddot{q}}{(T_{surf} - T_w)} = 121.5\ (kW/m^2\ K)$$

RESULTS AND DISCUSSION

4.1 Introduction

This investigation, as mentioned before is aimed to study experimentally the influence of local forced convective heat transfer to boiling flow (two phase flow). An experimental work has been designed using simple test rig.

This chapter represents the discussion of the experimental results about the influence of flow temperature and flow rate on single phase, void fraction on the flow, water temperature on the heat transfer coefficient, void fraction on temperature difference (T_{surf} - T_w), and relation between heat transfer coefficient and temperature different between(T_{surf} - T_w). Measured parameters and results parameters are shown in appendix (A).

4.2 Influence of Flow Temperature and Flow Rate

The influence of flow temperature and flow rate on single phase heat transfer coefficients are studied and the data of the experiments show that the heat transfer coefficient at constant flow rate is constant for some time when the heat flux is constant, then starts to increase, this is because at that point the heat flux starts to increase with increasing flow temperature as shown in figure (4.1). Also the increase of the volume flow rate at constant heat flux decreases the temperature difference between the wet end surface of the heating probe and the flow, therefore the heat transfer coefficient increases with the increase of the volume flow rates as shown in figure (4.2).

$$h = \frac{\ddot{q}}{\Delta T}$$

There is a possibility of using the heat transfer (heating probe) as flow meter for measuring flow rates at constant flow temperature and constant heat flux.

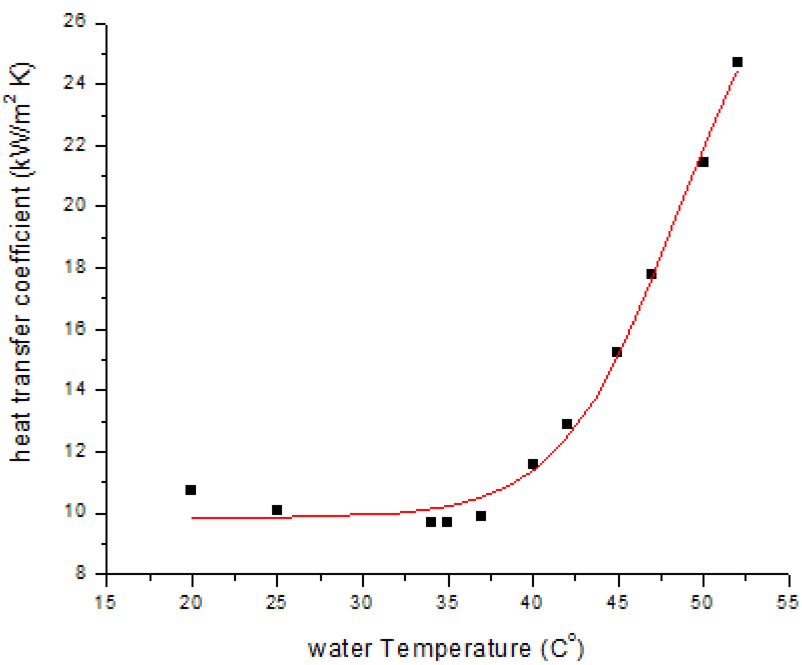

Fig (4.1) the relation between heat transfer coefficient and water temperature at constant volume flow rate (24 L/min).

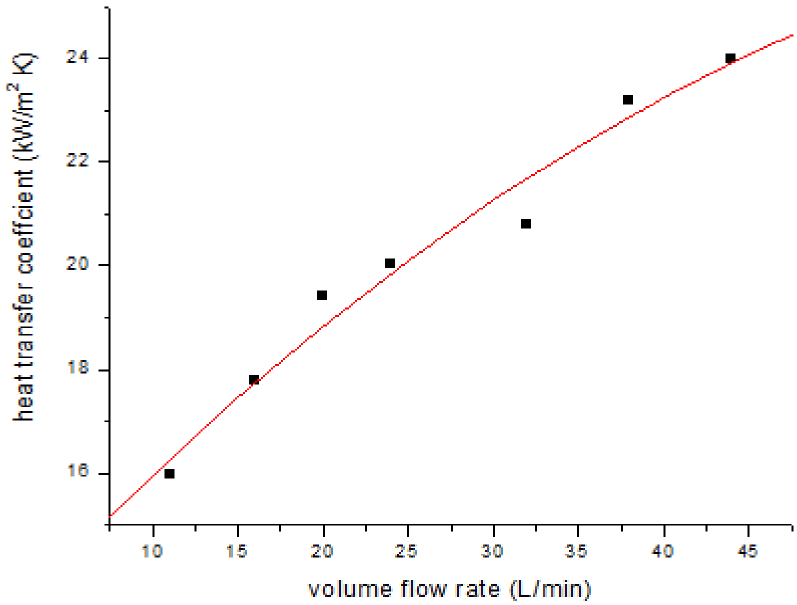

Fig (4.2) the relation between heat transfer coefficient and different volume flow rate.

4.3 Influence of Void Fraction in the Flow:

A number of experiments are curried out for a flow rates 24 and 30 l/min with different void fractions in the flow, and different heat flux. The data is represented in tables (see appendix A) and figures (4.3),(4.4). They show that the increase of void fraction in the flow increases the heat transfer coefficients. This is because the formation of the bubbles in the flow causes a turbulence in the flow and the increase of the void fraction increases the turbulence.

The flow is not bubble flow only, the bubble flow void fraction up to 20% after that the flow is plug flow up to 50% (see photos in the appendix B).

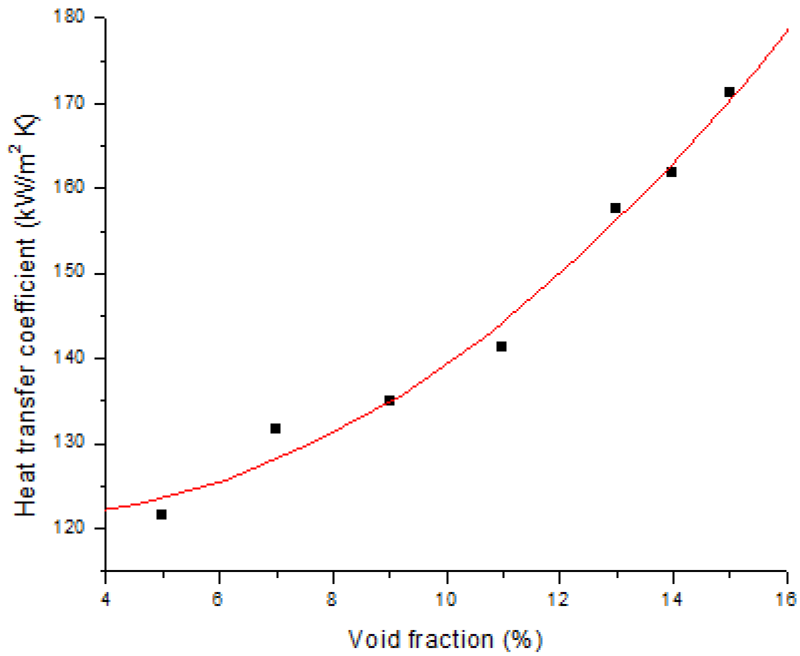

Fig (4.3) influence of void fraction on heat transfer coefficient at volume flow rate(24 L/min).

In general the flow was not bubble (flow only), the bubbly flow void fraction starts in boiling temperature but is not the same at different volume flow rate

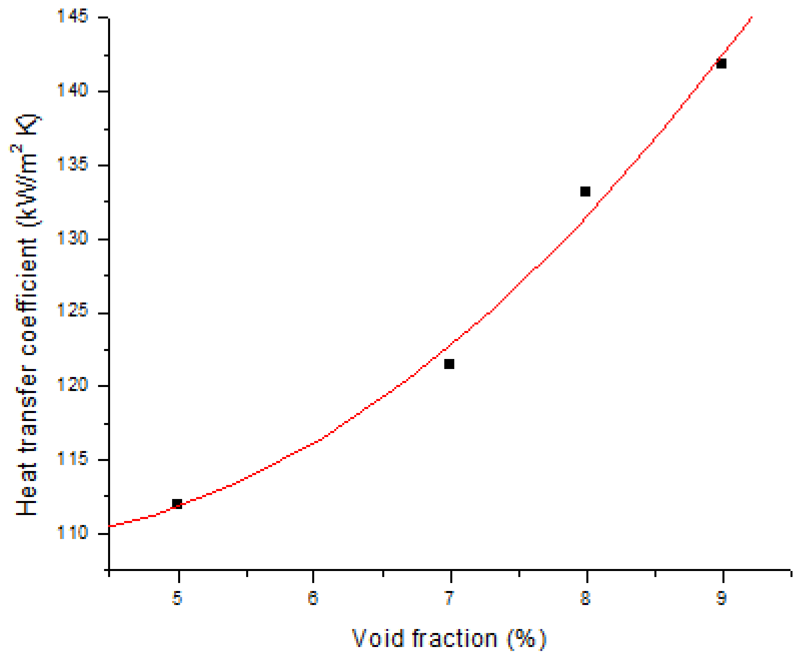

Fig (4.4) influence of void fraction on heat transfer coefficient at volume flow rate(30 L/min).

4.4 Influence of Water Temperature on the Heat Transfer Coefficient:

Fig (4.5), (4.6), (4.7) shows the behavior of the heat transfer coefficient (kW/m^2 K) with water temperature, at different flow rates (L/min). This is means that when the water temperature increases the heat transfer coefficient increases. The increase of the water temperature above the boiling temperature of the flow causes the void fraction.

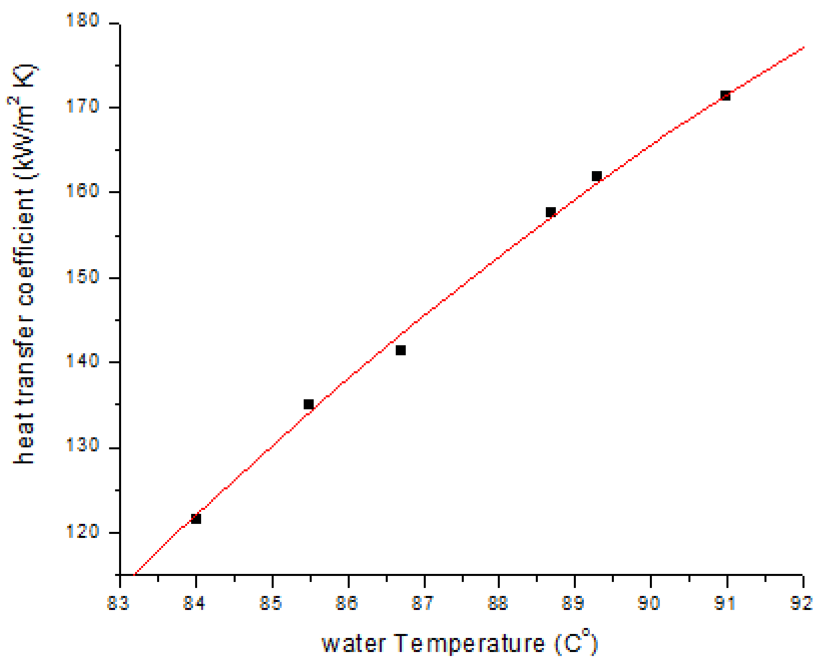

Fig (4.5) the relation between heat transfer coefficient and water temperature at constant volume flow rate (24 L/min).

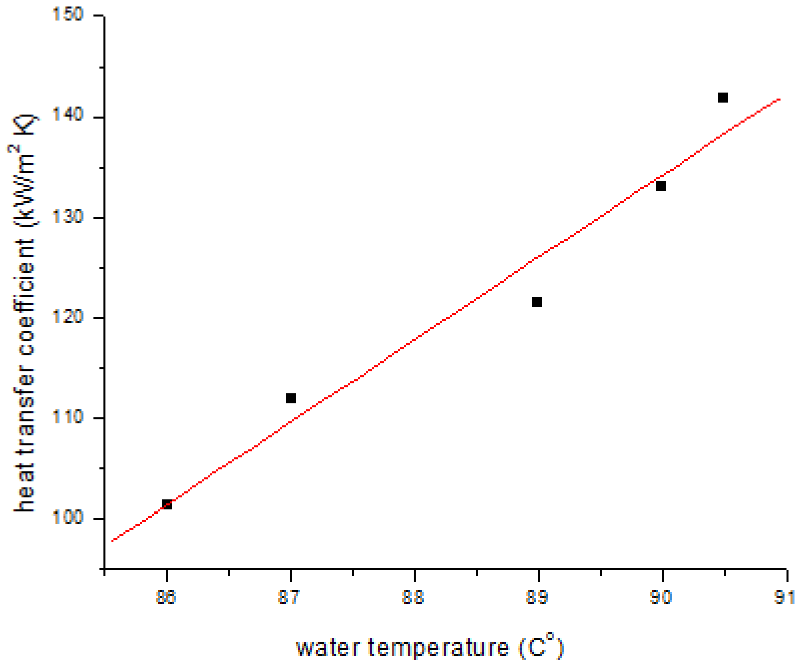

Fig (4.6) the relation between heat transfer coefficient and water temperature at constant volume flow rate (30 L/min).

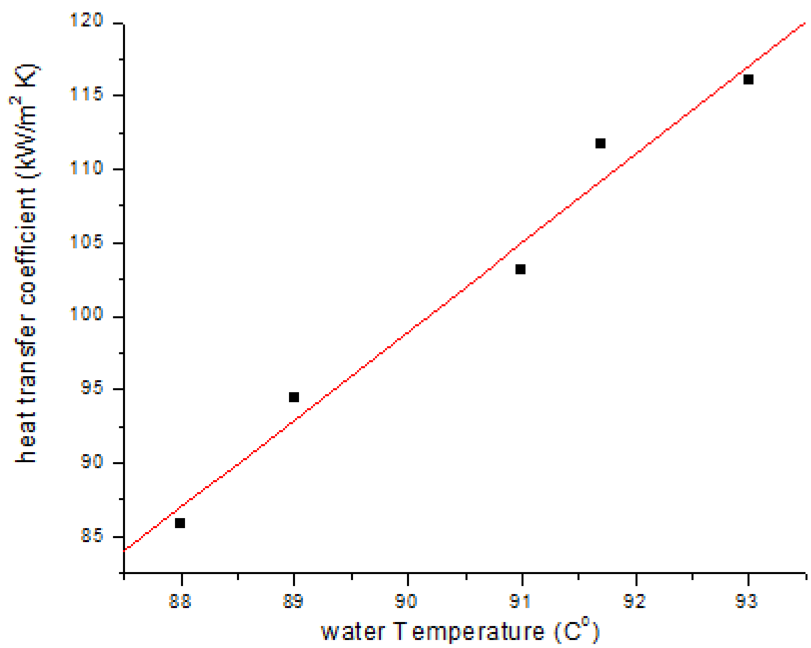

Fig (4.7) the relation between heat transfer coefficient and water temperature at constant volume flow rate (35 L/min).

4.5 Relation Between the Heat Transfer Coefficient and Temperature Different Between (T_{surf} -T_w):

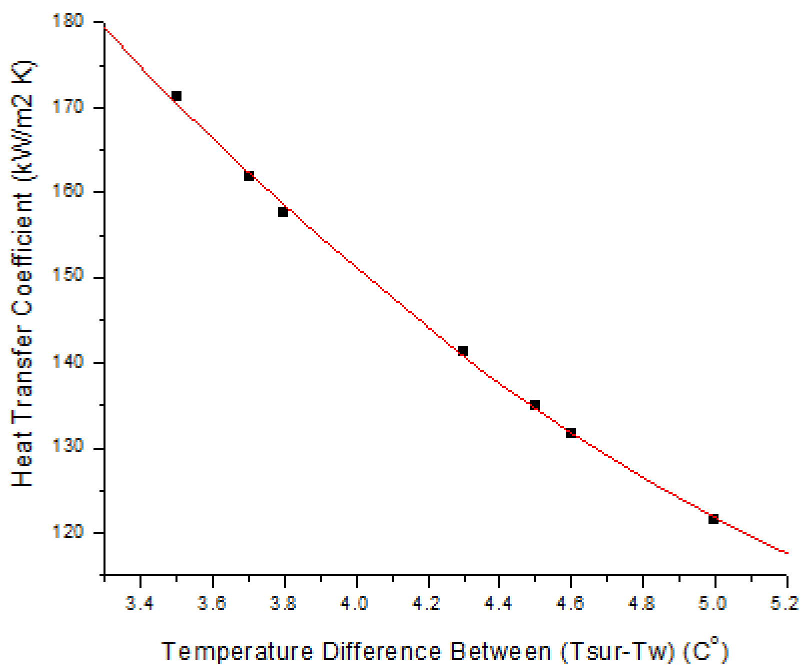

Fig(4.8) the relation between heat transfer coefficient and temperature different between (T_{surf} -T_w) at volume flow rate (24L/min)

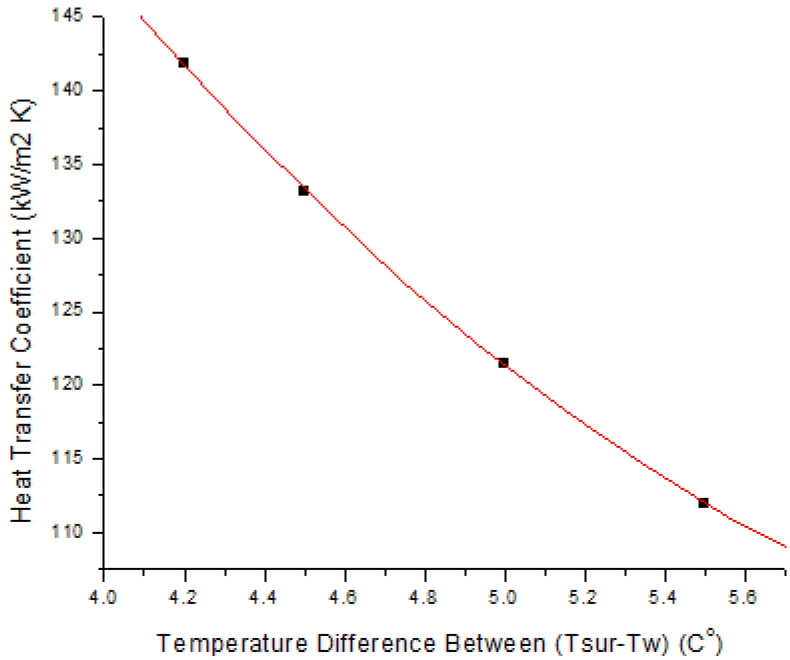

Fig(4.9) the relation between heat transfer coefficient and temperature different between (T_{surf} - T_w) at volume flow rate (30L/min)

4.6 Influence of Void Fraction on Temperature Difference (T_{surf} -T_w):

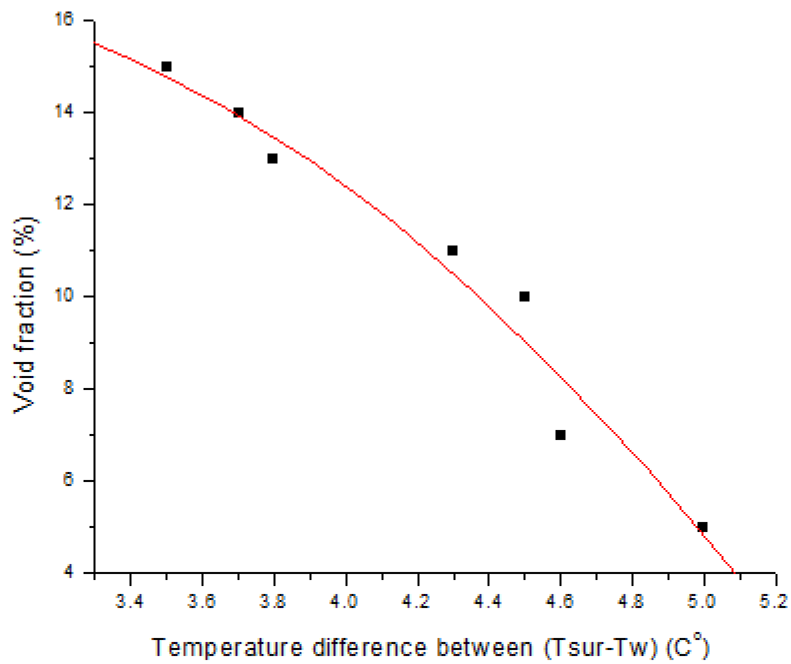

Fig(4.10) the relation between void fraction and temperature difference (T_{surf} -T_w) at volume flow rate (24L/min)

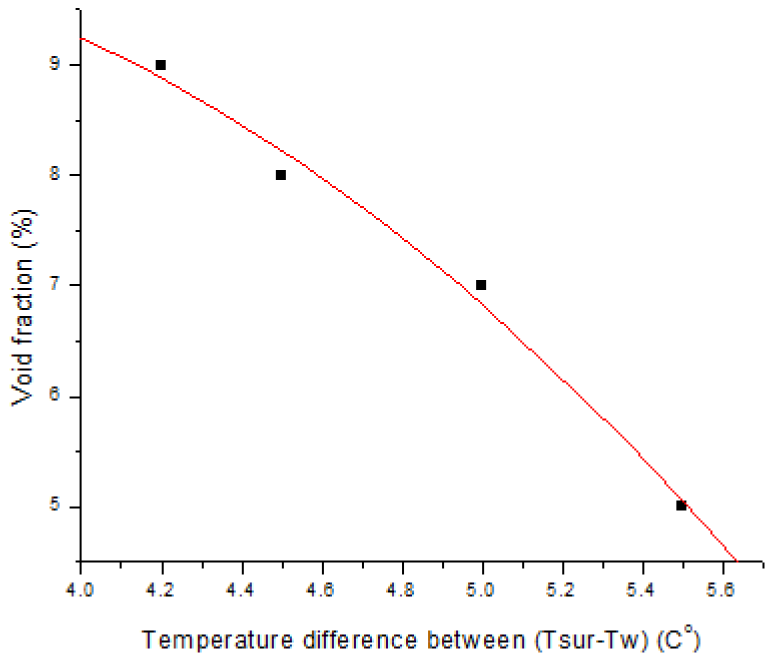

Fig(4.11) the relation between void fraction and temperature difference (T_{surf} -T_w) at volume flow rate (30L/min).

4.7 Influence of Void Fraction in the Flow at Volume Flow Rate (24 & 30 L/min):

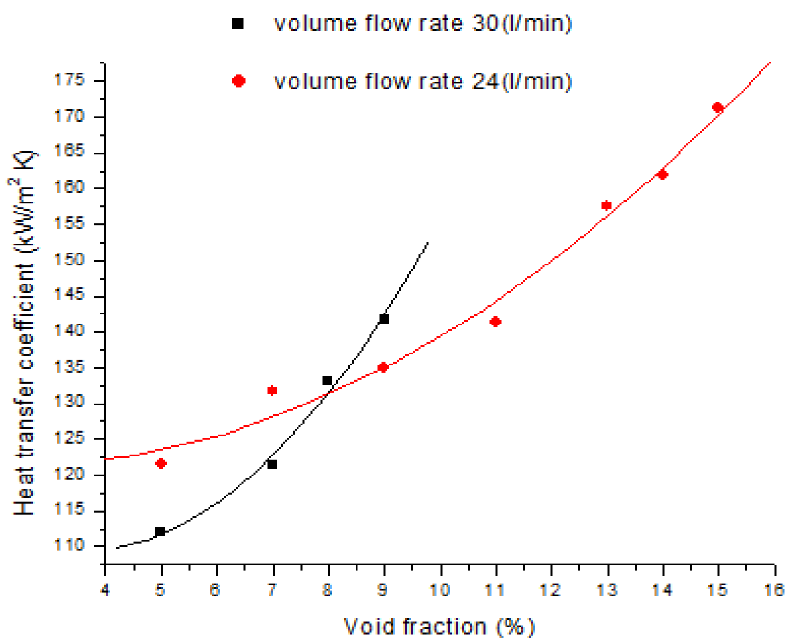

Fig (4.12) influence of void fraction on heat transfer coefficient at volume flow rate(24 & 30 L/min).

4.8 Relation Between the Heat Transfer Coefficient and Temperature Different Between (T_{surf} -T_w)

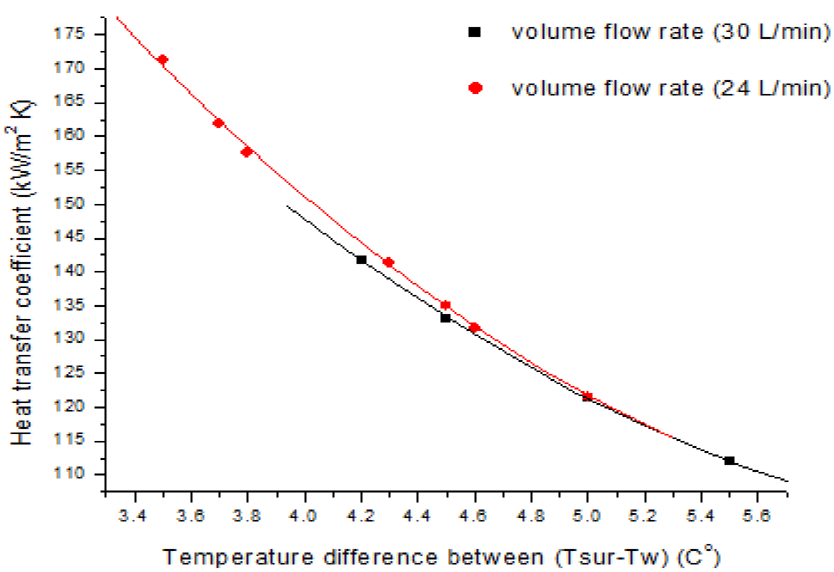

Fig(4.13) the relation between heat transfer coefficient and temperature different between (T_{surf} - T_w) at volume flow rate (24 & 30 L/min)

4.9 Influence of Void Fraction on Temperature Difference (T_{surf} -T_w) at Volume Flow Rate (24 & 30 L/min):

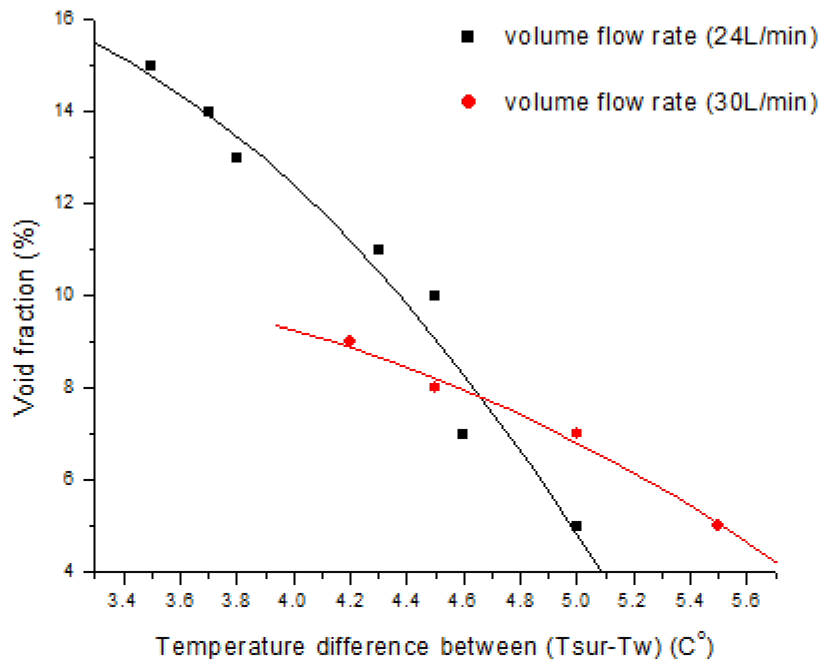

Fig(4.14) the relation between void fraction and temperature difference (T_{surf} -T_w) at volume flow rate (24 & 30 L/min)

CONCLUSIONS

Experimental studies are curried out to investigate Local boiling convective heat transfer coefficients are determine experimentally by using the flow boiling test rig. From the results the conclusions are as the followings:-

1. The heat transfer coefficients for single phase is constant at constant heat flux, and increases with the increase of heat flux.
2. The heat transfer coefficients for two phase flow increases with the increase of void fraction in the boiling flow. Also the heat transfer coefficients increase with the increase of heat flux.
3. The increase of the water temperature above the boiling temperature of the flow causes the void fraction, in sequence increase the heat transfer coefficients.
4. There is a possibility of using the heat transfer (heating probe) as flow meter for measuring flow rates of single phase flow at constant heat flux. But not for two phase.
5. The flow is bubble flow only at void fraction up to 20% after that the flow is plug flow up to 50%.
6. The heat transfer coefficients of two phase flow is increased by the decrease of the difference between water temperature and wet end surface temperature of the heating probe.
7. The temperature difference between water and wet end surface temperature of the heating probe decrease with the increases of void fraction.

REFERENCES

1. Arirachakaran, S. "An Experimental Study of Two-Phase Oil-Water Horizontal Pipes", M.S. Thesis, University of Tulsa (1983).
2. Claudi, M. C., Doctoral Thesis, "Flow Boiling Heat Transfer in Single Vertical Channels of Small Diameter", Stockholm, Sweden 2010.
3. Kandlikar S. G., Chung J. N, Multiphase Flow Handbook, CRC Press, Taylor and Francis Group (2006) Boiling and Condensation Chapter 3.
4. Collier, J. G., and J. R. Thorne, "Convective Boiling and Condensation", 3rd ed., pp. 170, 175، McGraw-Oxford Univ. Press, London & New York 1994.
5. Oshimowo, T., and M . E. Charles, 1974, Vertical Two-Phase Flow, I . Flow Pattern Correlation, Can. J Chem. Eng. 52:25-35.
6. V. G. Nino, P. S. Hrnjak, T. A. Newell, Characterization of Two-Phase Flow in Micro Channels, ACRC TR-202 (October 2002).
7. Tong, L. S., Tong, Y. S., "Boiling Heat Transfer and Two-Phase Flow", Taylor & Francis, America (1997).
8. Buongiorno, J., Notes, "Two-Phase Flow Boiling Heat Transfer and Boiling Crises in PWRs and BWRs", (2010).
9. Hewitt, G. F., “Fluid Mechanics Aspects of Two-Phase Flow, in S. G. Kandlikar, M. Shoji, and V. K. Dhir (eds.), Handbook of Boiling and Condensation, Chap. 9, Taylor and Francis, New York, 1999.
10. Mishima, K., and Hibiki, T., “Some Characteristics of Air-Water Two-Phase Flows in Small Diameter Tubes”, Int. J. Multiphase Flow, vol. 22, no. 4, pp. 703–712, 1996.

11. Bonjour, J,. and Lallemand, M,. "Flow Patterns during Boiling in a Narrow Space between Two Vertical Surfaces", Lnt. J. Multiphase Flow, vol. 24 pp 947-960, 1998.
12. Hetsroni, G., Segal, Z., and Mosyak, A., "Non-uniform Temperature Distribution in Electronic Devices Cooled by Flow in Parallel Micro-channels", Packaging Electronic Photonic Devices, EEP-vol. 28, pp. 1–9, 2000.
13. Lin, S., Kew, P. A., and Cornwell, K., “Two-Phase Flow Regimes and Heat Transfer in Small Tubes and Channels”, Heat Transfer 1998, Proc. 11th Int. Heat Transfer Conf., Kyongju, Korea, 1998, vol. 2, pp. 45–50.
14. kandliker, S. G., Steinke, M. E., Tian, S., and Campbell, L. A., "High-Speed Photographic Observation of Flow Boiling of Water in Parallel Mini-Channels, ASME Natl" . heat transfer conf., june 2001.
15. Cornwell, K., and Kew, P. A. ,"Boiling in Small Parallel Channels", Proc CECConf on Energy Ef. Ciency in Process Technology, Athens, Greece, October 1992, Elsevier Applied Sciences, pp. 624-638.
16. Lin, S., Kew, P. A., and Cornwell, K., "Two-Phase Evaporation in a 1mm Diameter Tube", 6th UK Heat Transfer Conf. in Edinburgh, September 1999.
17. Wambsganss, M. W., France, D. M., Jendrzejczyk, J. A., and Tran, T. N., "Boiling Heat Transfer in Small Diameter Tube", ASME J. Heat Transfer, vol. 115, no. 4, pp. 963-972, 1992.
18. Mertz, R. ,Wein, A., and Groll, M., "Experimental Investigation of Flow Boiling Heat Transfer in Narrow Channels", Calore e Technologia, vol. 14, no. 2, pp. 47-54, 1996.

19. Rivera W., and Xicale A. "Heat Transfer Coefficients in Two Phase Flow for the Water/Lithium Bromide Mixture Used in Solar Absorption Refrigeration Systems" Solar Energy Materials and Solar Cells 70 (2001) 309-320.
20. Karsli S, Yilmaz M., Comakli O. "The effect of internal surface modification on flow instabilities in forced convection boiling in a horizontal tube" International Journal of Heat and Fluid Flow 23 (2002) 776–791.
21. Ghiaasiaan S. M., Chedester R. C. "Boiling incipience in micro channels" International Journal of Heat and Mass Transfer 45 (2002) 4599–4606.
22. Qu,W., and Mudawar, I., "Flow Boiling Heat Transfer in Two Phase Micro-Channel Heat Sinks", International Journal of Heat and Mass Transfer 46 (2003) 2755–2771.
23. Wang C. C., Chen I. Y., Yang Y. W., Chang Y. J. "Two-phase flow pattern in small diameter tubes with the presence of horizontal return bend" International Journal of Heat and Mass Transfer 46 (2003) 2975–2981.
24. Hibiki, T., Ishi, M., "One Dimensional Drift-Flux Model for Two-Phase Flow in a Large Diameter Pipe", International Journal of Heat and Mass Transfer 46 (2003) 1773–1790.
25. Huai, X., Koyama, S., Zhao, T. S., Shinmura, E., Hidehiko, K., and Masaki, M., "Experimental Study of Flow Boiling Characteristics of Carbon Dioxide in Multiport Mini Channels", Journal International accepted 15 October 2003, Available online 5 January 2004, Applied Thermal Engineering 24 (2004) 1443–1463.
26. Lee, J., and Mudawar, I., "Two Phase Flow in High-Heat-Flux Micro-Channel Heat Sink for Refrigeration Cooling Applications", International Journal of Heat and Mass Transfer 48 (2005) 941–955.

27. Changhong, P., Yun, G., Suizheng, Q., Dounana, J., and Changhua, N. ,"Two Phaes Flow and Boiling Heat Transfer in Two Vertical Narrow Annuli", International Journal in Multiphase Flow 22, 703-712.
28. Hetsroni, G., Mosyak, A., Pogrebnyak, E., Segal, Z., "Explosive Boiling of Water in Parallel Micro-Channels",International Journal of Multiphase Flow 31 (2005) 371-392.
29. Changhon, p., Yun, G., Suizheng, Q., Dounan, J., Changhua, N. ,"Two-Phase Flow and Boiling Heat Transfer in Two Vertical Narrow Annuli", International Journal in Multiphase Flow 22, 703-712.
30. Owahib, w. , "Experimental Heat Transfer, Pressure Drop, and Flow Visualization of R-134a in Vertical Mini/Micro Tubes", Doctoral Thesis Stockholm, Sweden 2007.
31. Krishnamurthy S., and Peles, Y. “Flow Boiling of Water in a Circular Staggered Micro-pin Fin Heat Sink” International Journal of Heat and Mass Transfer 51 (2008) 1349–1364.
32. Basu, S., Ndao, S., Michna, G. J., Peles, Y., Jensen, M. K., "Flow Boiling of R134a in Circular Micro-tubes Part II: Study of Critical Heat Flux Condition", International Journal of Heat Transfer 2011 by ASME MAY 2011, Vol. 133 / 051503-1.

Volume flow rate (24 L/min)

T_1 (C°)	T_2 (C°)	T_w (C°)	r	T_{surf} (C°)	$(T_{surf} - T_w)$ (C°)	k (W/m K)	Δx (m^2)	q (W/m^2)	h (kW/m^2 K)	α (%)
162	125	84	0.5	89	5	270	0.016	607500	121.5	5
162.4	125.5	85	0.5	89.6	4.6	270	0.016	605812.5	131.7	7
162	126	85.5	0.5	90	4.5	270	0.016	607500	135	9
163	127	86.7	0.5	91	4.3	270	0.016	607500	141.3	11
163.5	128	88.7	0.5	92.5	3.8	270	0.016	599062.5	157.6	13
164	128.5	89.3	0.5	93	3.7	270	0.016	599062.5	161.9	14
165.5	130	91	0.5	94.5	3.5	270	0.016	599062.5	171.2	15

Volume flow rate (30 L/min)

T_1 (C°)	T_2 (C°)	T_w (C°)	r	T_{surf} (C°)	$(T_{surf} - T_w)$ (C°)	k (W/m K)	Δx (m^2)	q (W/m^2)	h (kW/m^2 K)	α (%)
165.5	129	87	0.5	92.5	5.5	270	0.016	615937	111.988	5
166	130	89	0.5	94	5	270	0.016	607500	121.5	7
165.5	130	90	0.5	94.5	4.5	270	0.016	599062.5	133.125	8
165.3	130	90.5	0.5	94.7	4.2	270	0.016	595687.5	141.83	9

Volume flow rate (35 L/min)

T_1 (C°)	T_2 (C°)	T_w (C°)	r	T_{surf} (C°)	k (W/m K)	Δx m^2	q (W/m^2)	h (kW/m^2 K)
149.5	121.5	88	0.5	93	270	0.016	472500	85.9
150	122	89	0.5	94	270	0.016	472500	94.5
150.5	123	91	0.5	95.5	270	0.016	464062.5	103.1
151.5	123.7	91.7	0.5	95.9	270	0.016	469125	111.7
152	124.5	93	0.5	97	270	0.016	464062.5	116

Tables

Table (A.1) heat transfer coefficient correlation and water temperature at constant volume flow rate (24 L/min).

Water temperature (C^0)	Heat transfer coefficient ($kW/m^2\,K$)
20	10.76
25	10.08
34	9.67
35	9.67
37	9.91
40	11.56
42	12.9
45	15.21
47	17.79
50	21.45
52	24.72

Table (A.2) heat transfer coefficient correlations and different volume flow rate.

Different volume flow rate (L/min)	Heat transfer coefficient (kW/m^2 K)
44	24
38	23.2
32	20.8
24	20.04
20	19.4
16	17.8
11	15.98

Table (A.3) influence of void fraction on heat transfer coefficient at volume flow rate(24 L/min).

Void fraction (%)	Heat transfer coefficient (kW/m^2 K)
5	121.5
7	131.7
9	135
11	141.3
13	157.6
14	161.9
15	171.2

Table (A.4) influence of void fraction on heat transfer coefficient at volume flow rate(30 L/min).

Void fraction (%)	Heat transfer coefficient (kW/m^2 K)
5	111.988
7	121.5
8	133.125
9	141.83

Table (A.5) the relation between heat transfer coefficient and water temperature at constant volume flow rate (24 L/min).

Water temperature (C^0)	Heat transfer coefficient (kW/m^2 K)
84	121.5
85.5	135
86.7	141.3
88.7	157.6
89.3	161.9
91	171.2

Table (A.6) the relation between heat transfer coefficient and water temperature at constant volume flow rate (30 L/min).

Water temperature (C^0)	Heat transfer coefficient (kW/m^2 K)
80	63.1
81.5	70.5
86	101.3
87	111.99
89	121.5
90	133.1
90.5	141.8

Table (A.7) the relation between heat transfer coefficient and water temperature at constant volume flow rate (35 L/min).

water temperature (C^0)	Heat transfer coefficient (kW/m^2 K)
88	85.9
89	94.5
91	103.1

91.7	111.7
93	116

Table (A.8) the relation between heat transfer coefficient and temperature different between (T_{surf} -T_w)at volume flow rate (24L/min).

Heat transfer coefficient (kW/m^2 K)	Temperature different between (T_{surf} -T_w) (C^0)
121.5	5
131.7	4.6
135	4.5
141.3	4.3
157.6	3.8
161.9	3.7
171.2	3.5

Table (A.9) the relation between heat transfer coefficient and temperature different between (T_{surf} -T_w)at volume flow rate (30L/min).

Heat transfer coefficient (kW/m^2 K)	Temperature different between (T_{surf} -T_w) (C^0)
111.988	5.5
121.5	5
133.125	4.5
141.83	4.2

Table (A.10) the relation between temperature different between (T_{surf} -T_w) and void fraction at volume flow rate (24L/min).

Temperature different between (T_{surf} -T_w) (C^0)	Void fraction (%)
5	5
4.6	7
4.5	10

4.3	11
3.8	13
3.7	14
3.5	15

Table (A.11) the relation between temperature different between (T_{surf} -T_w) and void fraction at volume flow rate (30L/min).

Temperature different between (T_{surf} -T_w) (C^0)	Void fraction (%)
5.5	5
5	7
4.5	8
4.2	9

Photos

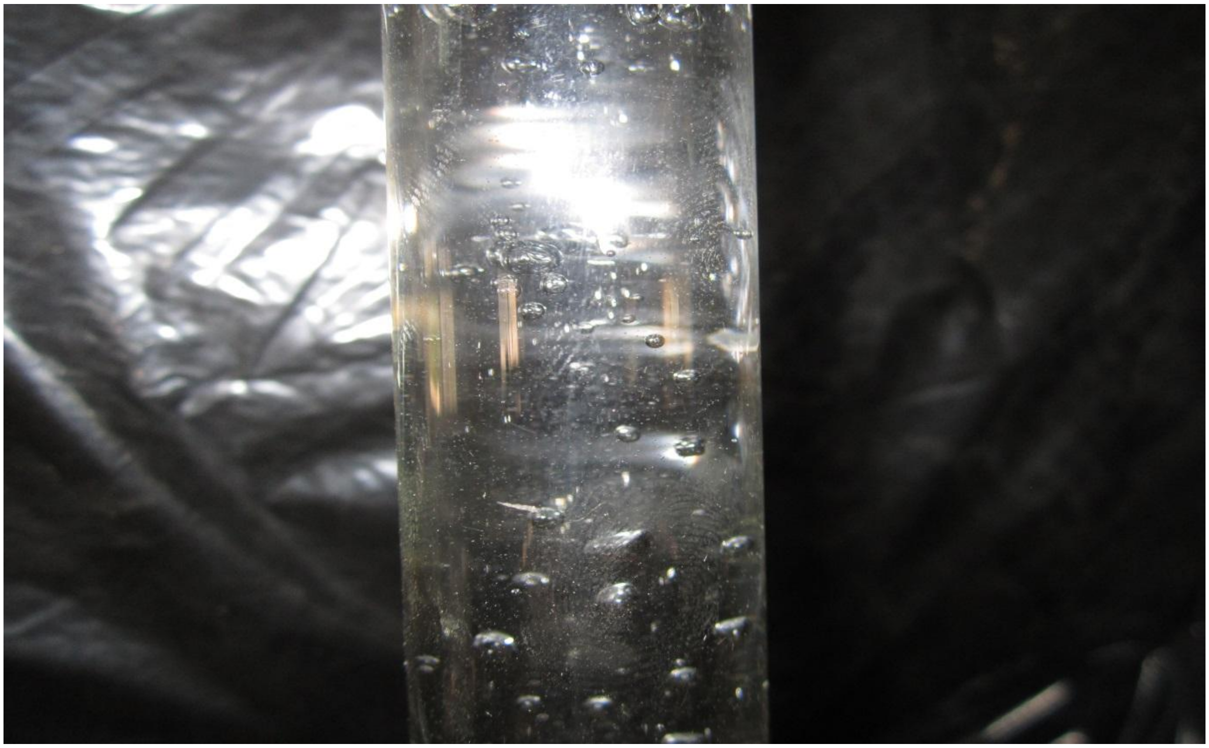

Photo (B-1) void fraction 5% at Volume flow rate (24).

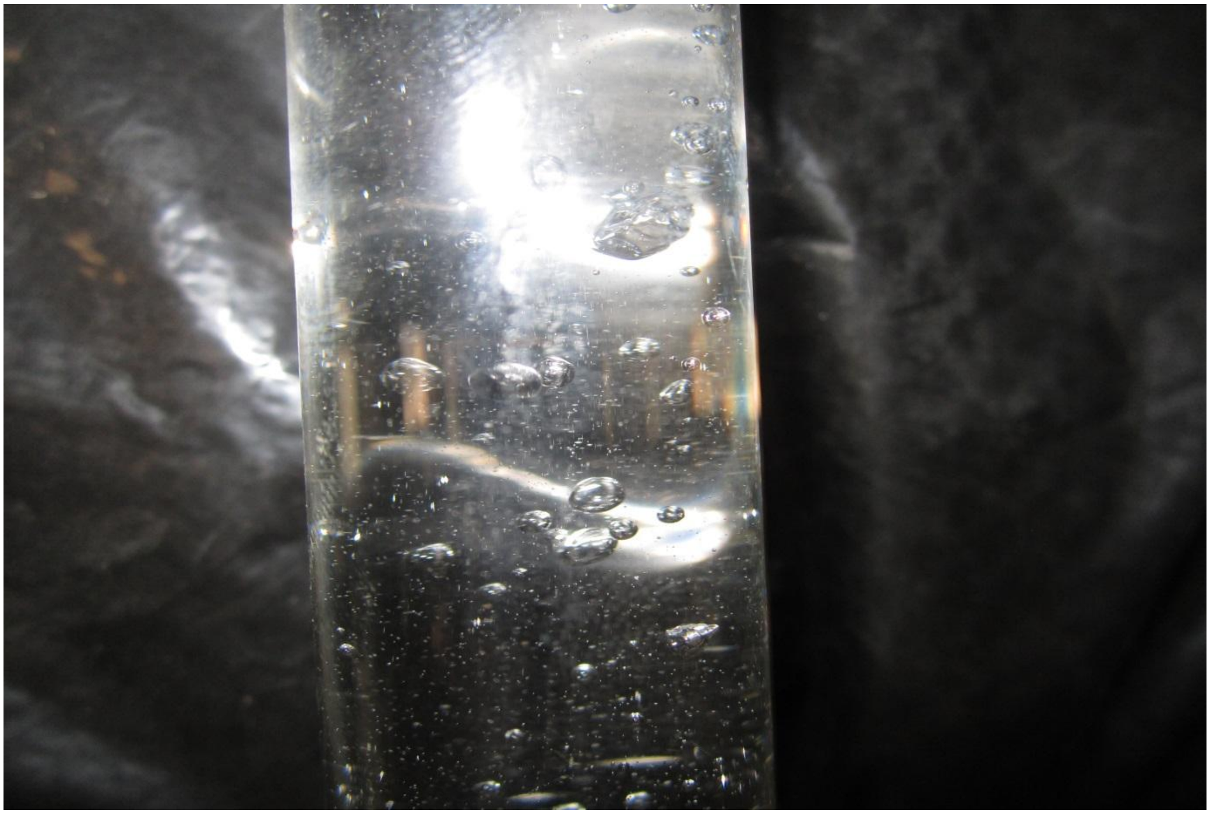

Photo (B-2) void fraction 7% Volume flow rate (24).

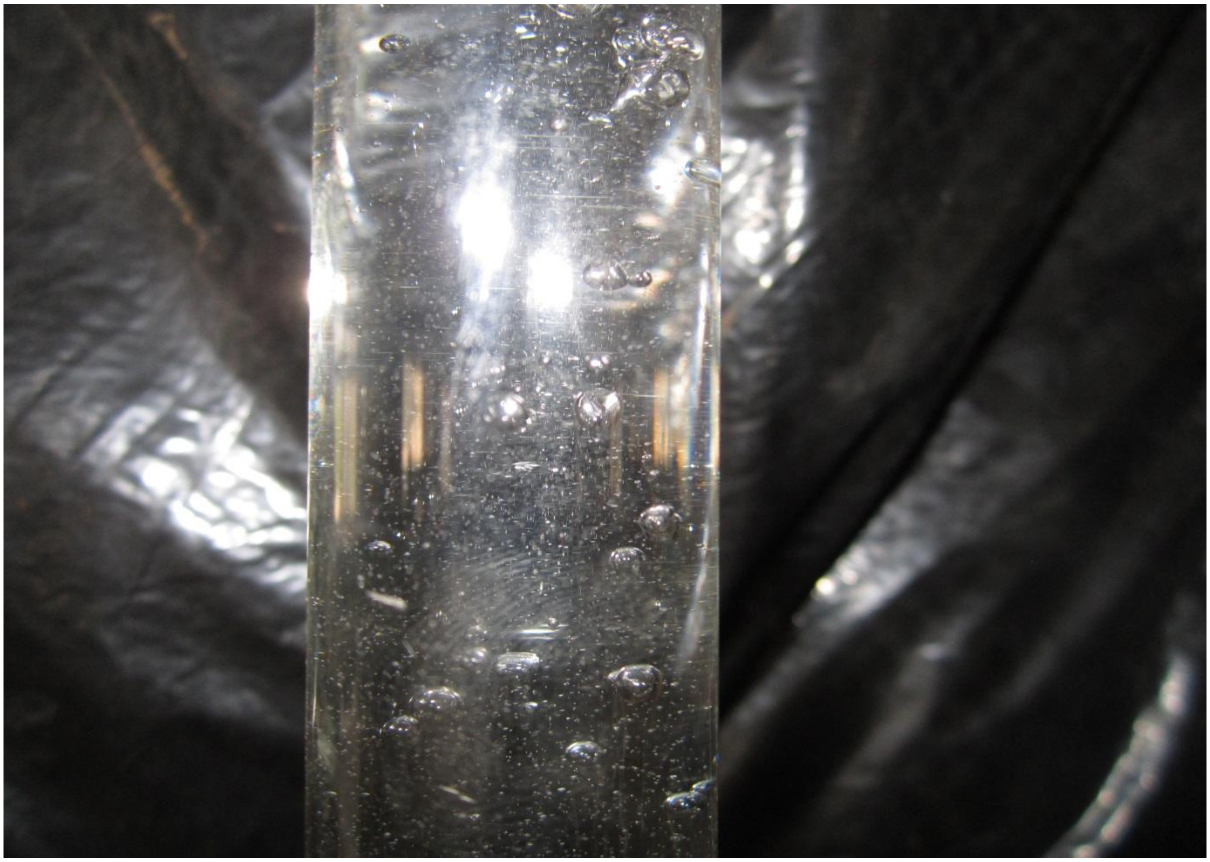

Photo (B-3) void fraction 9% Volume flow rate (24).

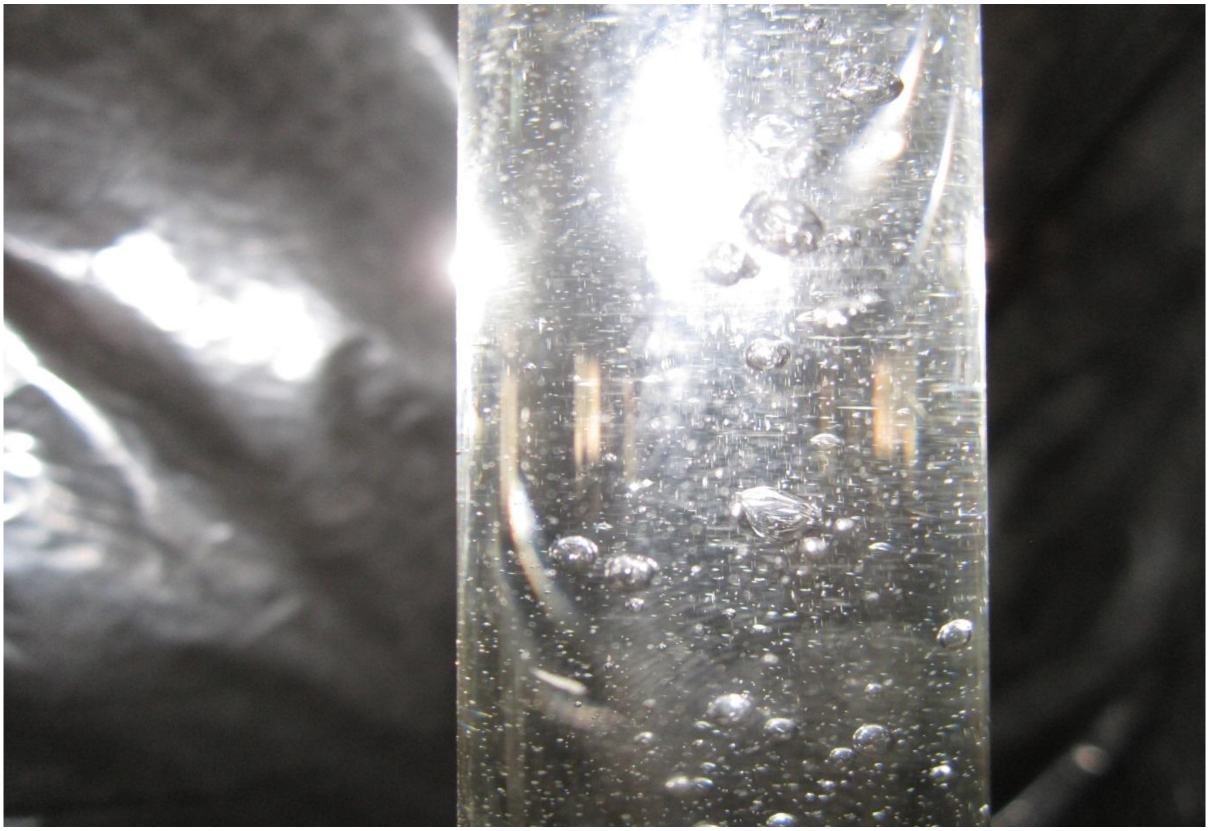

Photo (B-4) void fraction 11% Volume flow rate (24).

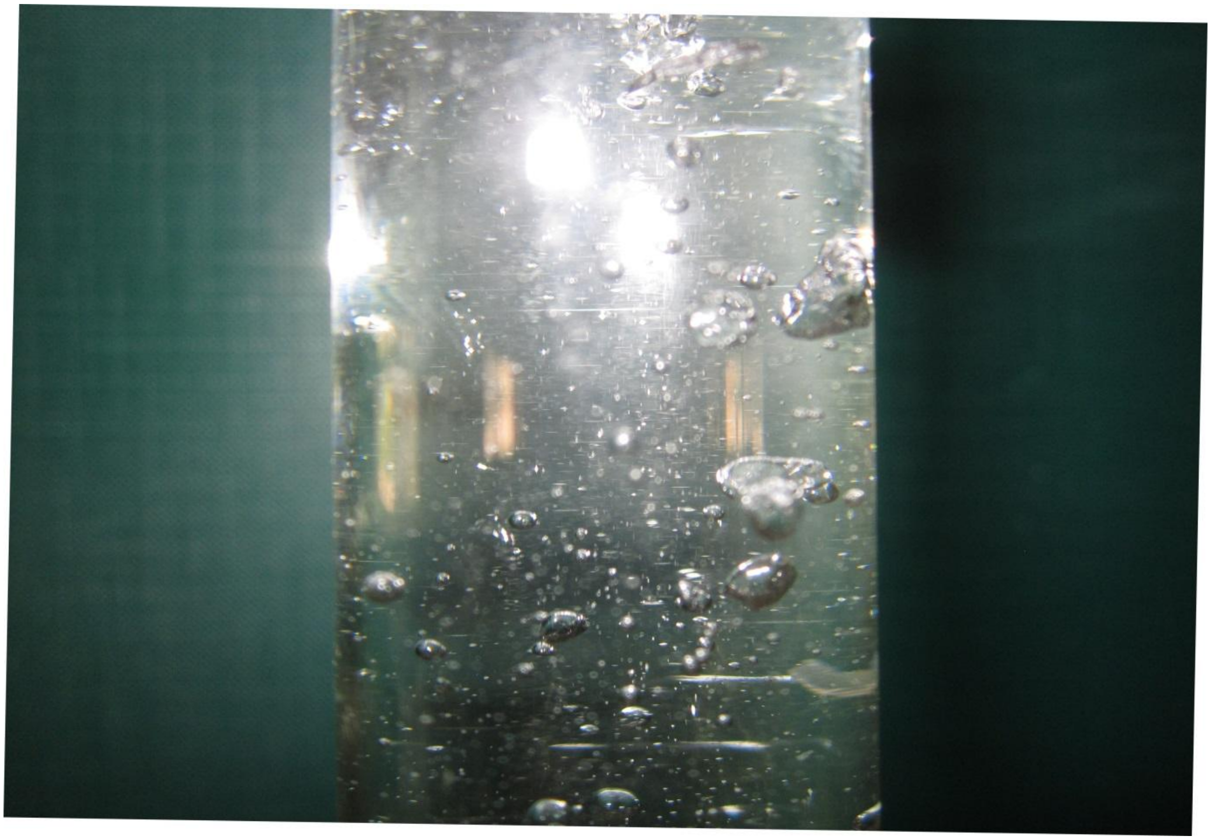

Photo (B-5) void fraction 13% Volume flow rate (24).

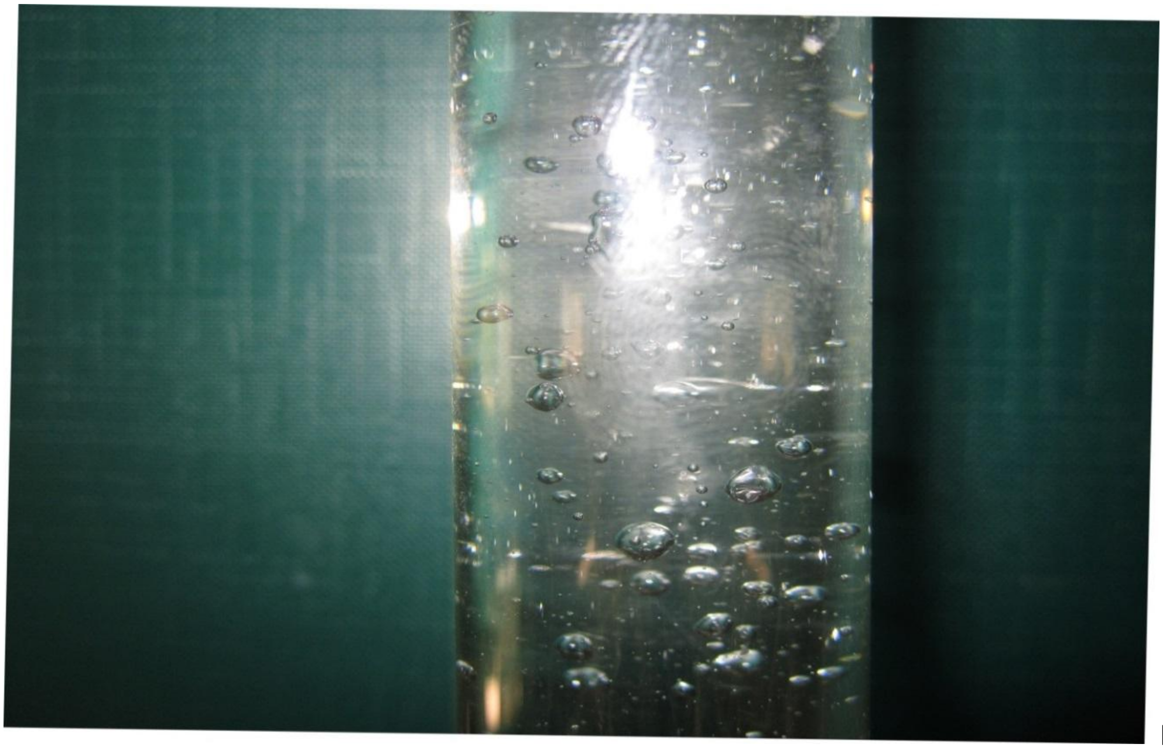

Photo (B-6) void fraction 14% Volume flow rate (24).

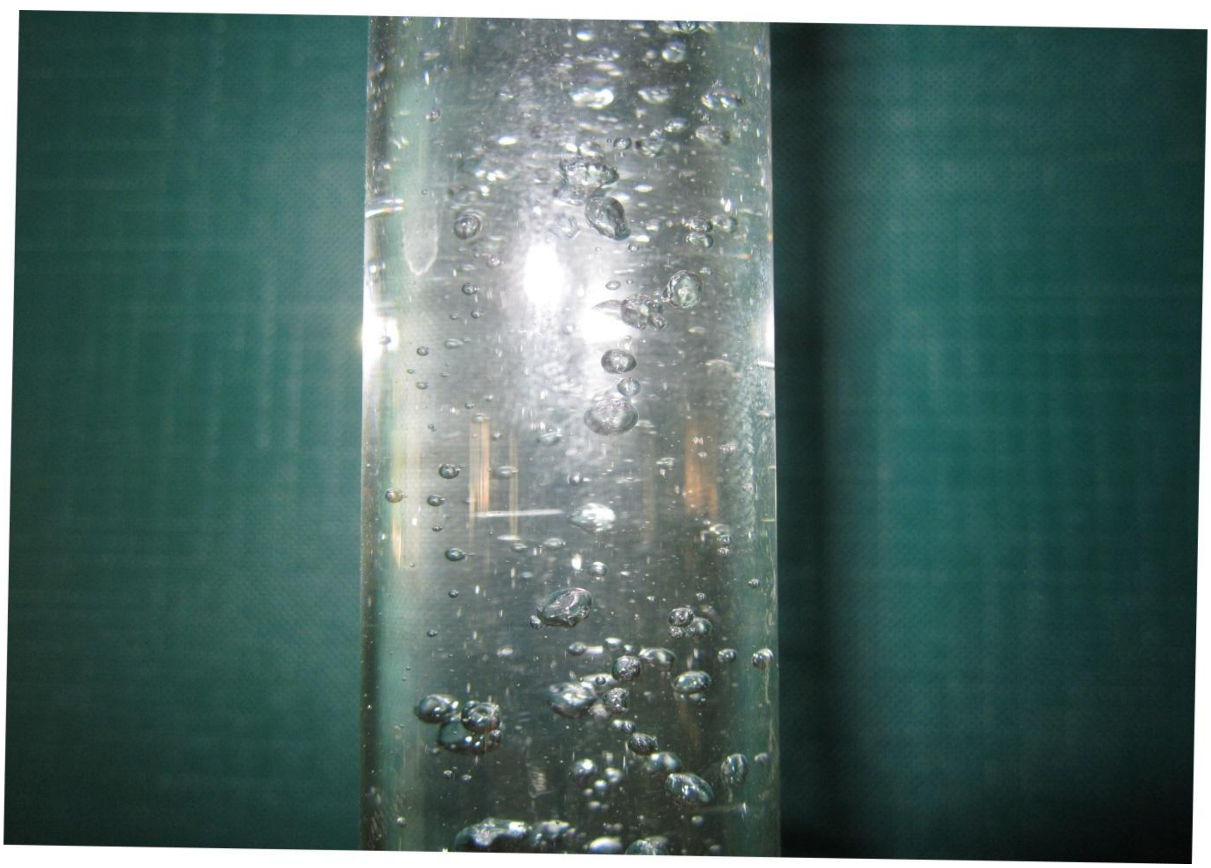

Photo (B-7) void fraction 15% Volume flow rate (24).

Photo (B-8) void fraction 5% at Volume flow rate (30).

Photo (B-9) void fraction 7% at Volume flow rate (30).

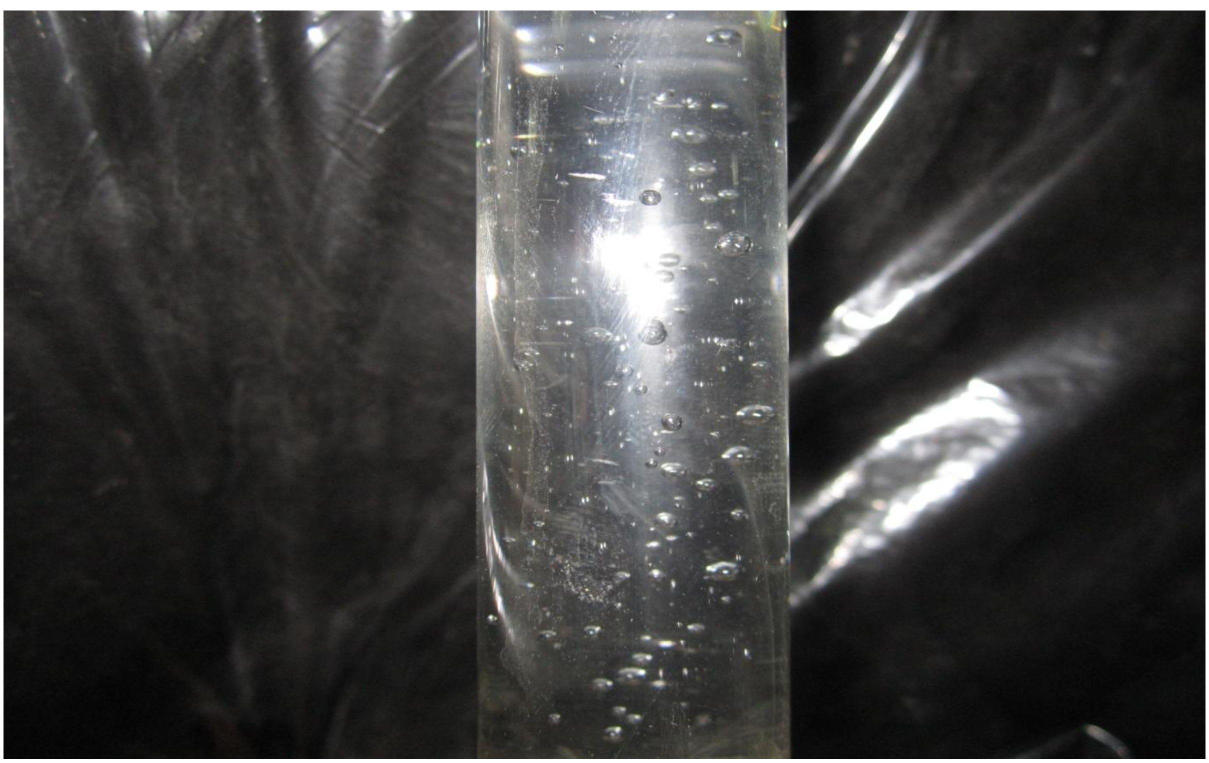

Photo (B-10) void fraction 8% at Volume flow rate (30).

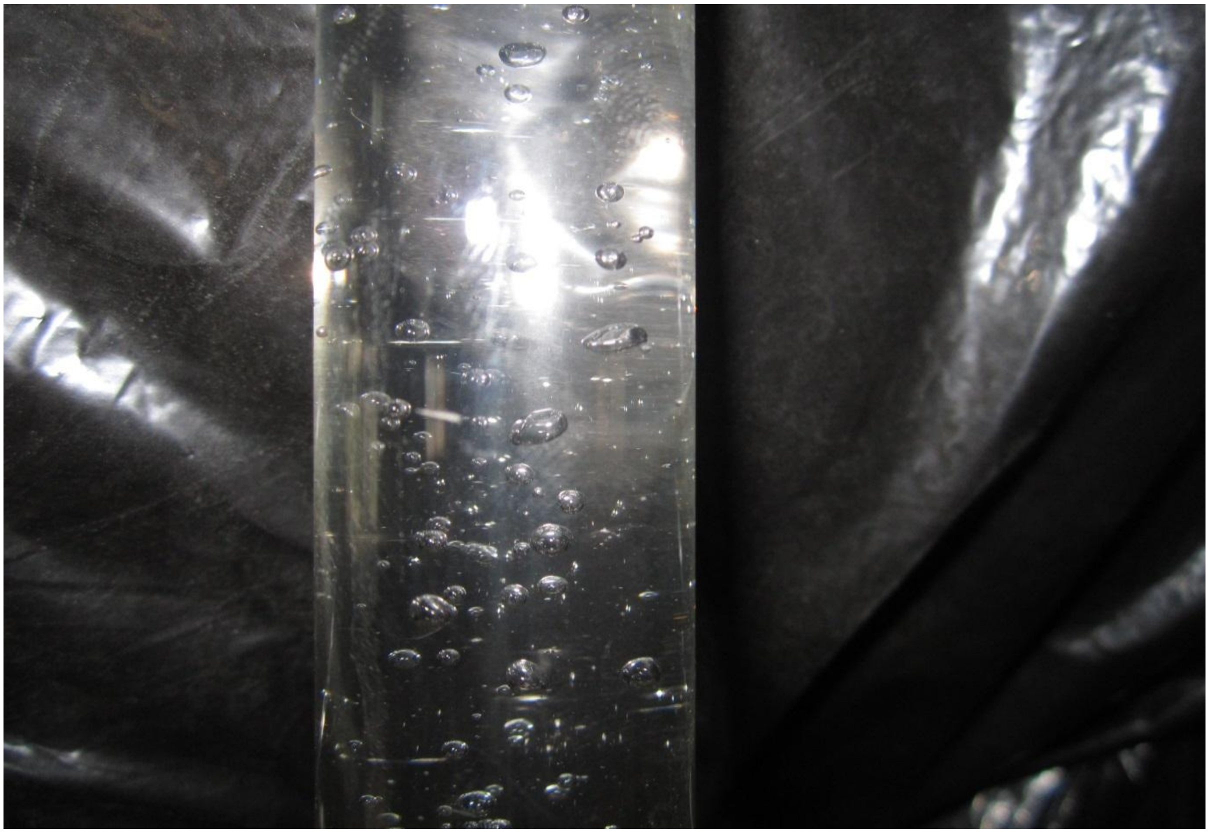

Photo (B-11) void fraction 9% at Volume flow rate (30).

Plug flow